Journal Pre-proof

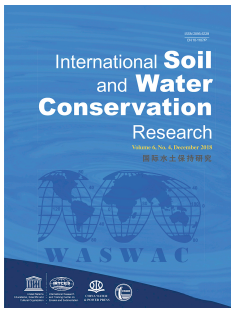

Analysis of rapidly decreasing discharge in the transboundary Amudarya River, Central Asia: considering climate change and human impacts

Rashid Mahmood, Shaofeng JIA, Mukand S. Babel, Zhipin AI, Shahid Naeem, Mujtaba Hassan, Jiabao Yan, Zhu Wenbin

PII: S2095-6339(26)00074-2

DOI: https://doi.org/10.1016/j.iswcr.2026.100682

Reference: ISWCR 100682

To appear in: *International Soil and Water Conservation Research*

Received Date: 1 July 2025

Revised Date: 6 June 2026

Accepted Date: 13 June 2026

Please cite this article as: Mahmood R., JIA S., Babel M.S., AI Z., Naeem S., Hassan M., Yan J. & Wenbin Z., Analysis of rapidly decreasing discharge in the transboundary Amudarya River, Central Asia: considering climate change and human impacts, *International Soil and Water Conservation Research*, https://doi.org/10.1016/j.iswcr.2026.100682.

Analysis of rapidly decreasing discharge in the transboundary Amudarya River, Central Asia: considering climate change and human impacts

Rashid Mahmood[1], Shaofeng JIA[2], Mukand S. Babel[1], Zhipin AI[2] , Shahid Naeem[3], Mujtaba Hassan[4], Jiabao Yan[5], Zhu Wenbin[2]

[1] Water Engineering and Management, Asian Institute of Technology, Pathum Thani 12120, Thailand

[2] Institute of Geographic Science and Natural Resources Research, Chinese Academy of Sciences, Beijing 100101, China

[3] Regional Centre for Space Science and Technology Education in Asia and the Pacific (UN-affiliated), Beihang University, 3111150 Hangzhou Campus

[4] Department of Space Science, Institute of Space Technology, Islamabad Expressway, Islamabad, Pakistan

[5]Nanjing Institute of Environmental Sciences, Ministry of Ecology and Environment, Nanjing 210042, China

Correspondence to: Rashid Mahmood (rashi1254@gmail.com; rashid@ait.asia)

Author order:

1. Rashid Mahmood (rashi1254@gmail.com)
2. Shaofeng JIA (jiasf@igsnrr.ac.cn)
3. Mukand S. Babel (msbabel@ait.ac.th)
4. Zhipin AI (aizhipin@igsnrr.ac.cn)
5. Shahid Naeem (shahidn@igsnrr.ac.cn)
6. Mujtaba Hassan (mujtaba@grel.ist.edu.pk)
7. Jiabao Yan (jiabao.yan@foxmail.com)
8. Zhu Wenbin (zhuwb@igsnrr.ac.cn)

Analysis of rapidly decreasing discharge in the transboundary Amudarya River, Central Asia: considering climate change and human impacts

Abstract. The livelihoods of millions of people from five countries rely on the water resources of the transboundary Amudarya River basin, one of the most important freshwater systems in Central Asia. However, climate change (CC) and human activities (HA) have substantially altered the hydrological processes in the basin. This study provides one of the first comprehensive impact assessments of CC and HA on streamflow changes by analysing 90 years of simulated streamflow in this climate data-scarce region, using the hydrological modeling approach and climate elasticity. The data limitations were addressed by integrating multiple sources, including local and global datasets. The CC and HA's impacts were separately quantified at 29 sites across all the main Amudarya tributaries for 1951–2020 relative to 1931–1950. The results showed a substantial increase in temperature (0.51–0.83 °C) and precipitation (6–13%) in the entire basin. Streamflow decreased by 54–77% in the middle and lower reaches. Attribution analysis showed that human activities were the dominant driver of this decline, contributing 114–120% of the net reduction, while climate change partly offset the decline by increasing streamflow by 14–20%, mainly through increased precipitation. In the headwater region, streamflow decreased by 22%, with human activities contributing 140% of the net decline, offsetting the positive contribution from climate change. Major tributaries, including the Vakhsh, Kunduz, Kofirnihon, Surkhandarya, Zeravshan, and Qashqadarya, showed streamflow reductions of 4–34%, primarily attributed to HA. Climate elasticity revealed precipitation as the most sensitive element in the region, with an elasticity of 1.25. These latest and comprehensive findings provide valuable insights for improving water resources planning and management in the region under changing climatic and anthropogenic pressures.

Keywords: Amudarya River basin; Climate change; Human activities; Hydrological modelling; Freshwater resources; Climate elasticity; Central Asia

1 Introduction

Freshwater resources are essential for food production, energy generation, and domestic and industrial use, yet they are under increasing pressure from intensive human water withdrawals, particularly for irrigated agriculture (Singh et al., 2023; Sterner et al., 2020). Agriculture alone accounts for more than two-thirds of global water

extraction (Gilbert, 2012; Viala, 2008), and in several major river basins, including the Amudarya, extensive irrigation has severely reduced downstream flows (Mahmood and Jia, 2019). In parallel, climate change—marked by a global temperature increase of about 1.1 °C since pre-industrial times—has intensified hydrological extremes and increased risks to freshwater ecosystems (IPCC, 2022). The combined impacts of climate change and human activities on water resources vary substantially across regions, highlighting the need for basin-specific assessments (Mahmood and Jia, 2019)

The Amudarya River basin (ADRB) is the largest and most critical water resource in Central Asia and the main source of discharge to the Aral Sea. As a transboundary river, it flows through five countries: Afghanistan, Kyrgyzstan, Tajikistan, Turkmenistan, and Uzbekistan (UNEP, 2011), and supports the livelihoods of around 89 million people engaged in irrigated agriculture (Hou et al., 2023; Salehie et al., 2022b). Between 1950 and 1990, the Soviet Union established an extensive network of irrigation canals and pumping systems to promote regional socio-economic growth. This development led to a 150% increase in irrigated land within the ADRB, primarily to meet demand for crops such as wheat, rice, and cotton (World-Bank, 2004). Agriculture is a key contributor to the national Gross Domestic Product (GDP) in this region, but consumes 92% of the water withdrawn (Schlüter et al., 2013). For instance, during 2007–2008, agriculture comprised approximately 20% of the GDPs of Tajikistan, 25% of Turkmenistan, and over 28% of Uzbekistan (UNEP, 2003). This intense investment in irrigated agriculture has led to significant over-exploitation of freshwater resources, often with minimal regard for environmental preservation. These priorities have had, and continue to have, far-reaching impacts on the river's ecosystem. (UNEP, 2011). For example, since the 1960s, over 80% of the Aral Sea's surface area has disappeared, reducing its once-critical role in moderating the regional climate (He et al., 2022).

Additionally, the river's delta (28,500 km²) has also been severely impacted by decreasing streamflow due to agricultural expansion and dam construction, resulting in the loss of approximately 90% of the delta's Tugai forest since the 1930s (Schlüter et al., 2013). In addition, once a tributary of the Amudarya, the Zeravshan River is now largely diverted for human use, preventing it from reaching the river (Schlüter et al., 2013). Furthermore, climate change has noticeably impacted water resources in the ADRB. For example, evapotranspiration has increased by 62 mm since the 1960s, and most areas of the basin experience more precipitation but reduced streamflow at the outlet (Hu et al., 2021). Extreme alterations in the river flow regimes due to climate change and human activities have resulted in a lowered water table, extensive soil salinisation and desertification, significant reductions in fisheries in the Aral Sea, and glacier shrinkage (Kure et al., 2013). Thus, this compels us to separate and assess the impacts of climate change (CC) and human activities (HA) on streamflow patterns in the basin. Understanding

these impacts is crucial for developing effective regional water resource planning, management, and sustainable development strategies, ultimately ensuring a resilient and sustainable future for our communities.

Numerous studies, such as those by White et al. (2014), Salehie et al. (2022a), Immerzeel et al. (2012), Lioubimtseva (2014), and Wang et al. (2016), have been reported exploring the impacts of CC on water resources in the basin because of its dynamic importance in the region. However, a few studies have quantified the impact of CC and HA on water resources in the ADRB, i.e., Hu et al. (2021), Wang et al. (2020), Xu et al. (2021), and Hou et al. (2023). Among them, Xu et al. (2021) investigated the impacts of land use and climate change on streamflow using the hydrological modelling approach, but for future periods (i.e., 2021–2050). Wang et al. (2020) focused on determining the changes in the Aral Sea (i.e., surface area, water level, and water volume) from 1960 to 2018. They linked HA and natural parameters (i.e., temperature and precipitation) using a linear regression model to explore which factor affects the changes in the Ara Sea. However, they did not exclusively quantify the impacts of CC and HA on water resources. Hu et al. (2021) and Hou et al. (2023) are the only studies that exclusively quantified the impacts of CC and HA on Amudarya's water resources, using the Budyko framework and modelling approach, respectively. A key question in these studies concerns the selection of the baseline period (BLP): the first study uses 1960–1974 and 1960–2000, while the second uses 1956–1973. A BLP is the duration where the effects of human activities can be ignored. Although they used statistical methods to explore the change point, there are still doubts using these periods as BLPs because most of irrigation extraction and dam construction were accomplished during 1960–1990 (FAO, 2021; UNEP, 2011). Table S-1 (Supplementary Materials) provides a comprehensive list of dams and completion dates, such as the Karakum Canal, which, constructed in the 1960s and 70s, diverts approximately 15% of the Amudarya's flow near the Kerki discharge gauge (Brite, 2018). Additionally, their analyses focused only on three sites (i.e., Kelif, Kerki, and Kyzyl-jar) along the Amudarya excluding major tributaries like the Vakhsh, Panj, Kunduz, Surkhandarya, and Kofirnihon Rivers. To address these gaps, we separated and quantified the impacts of CC and HA on streamflow in the ADRB and all of its main tributaries (e.g., Vakhsh, Panj, Kunduz, Qashqadarya, Surkhandarya, and Kofirnihon Rivers) using the Hydrological Modelling Approach. Hydrological modelling provides a physically based framework that explicitly represents key hydrological processes, including snow and glacier melt, evapotranspiration, soil moisture dynamics, and groundwater–surface water interactions, making it particularly suitable for large, complex river basins. This approach has been widely applied and is considered robust for attributing streamflow changes to CC and HA (Chiew et al., 2006; Li et al., 2020). However, it requires detailed calibration and long-term hydroclimatic

time series, which are also essential for objectively defining an appropriate baseline period (BLP) (Mahmood and Jia, 2019).

In addition to attributing streamflow changes to CC and HA, it is critical to understand the sensitivity of streamflow to specific climatic variables, such as precipitation, temperature, and evapotranspiration, particularly in basins strongly influenced by snowmelt and glacier dynamics. The climate elasticity of streamflow provides a dimensionless, physically interpretable measure that quantifies the proportional response of river discharge to changes in climatic drivers(Anderson et al., 2024; Yang and Yang, 2011). To the best of our knowledge, Hu et al. (2021) is the only study that applied the climate elasticity method coupled with the Budyko framework to analyze streamflow change in the ADRB quantitatively. However, the selected BLP for this study is also questionable, as most water extractions occurred during these periods, as discussed above. Moreover, the Budyko method does not account for the impacts of groundwater storage, soil moisture, snow/glacier melting, and other cryospheric components within a basin, rendering it physically deficient for application in most catchments (Zheng et al., 2009). Different methods have been used to quantify climate elasticity, grouped into five categories by Sankarasubramanian et al. (2001): hydrological modelling, analytical, empirical, and statistical methods. Similar to quantifying impacts of CC and HA, we also used the hydrological modelling approach as the primary method, complemented by statistical analyses, to assess the climate elasticity of streamflow to precipitation, temperature, and evapotranspiration. The modelling approach was adopted as the primary method due to the strong influence of snow and glacier melt processes, and because it is widely used and enables process-based evaluation of streamflow sensitivity under controlled climate perturbations (Chiew et al., 2006). On the other hand, the statistical indicators proposed by Sankarasubramanian et al. (2001) and Zheng et al. (2009) were used as complementary analyses to examine consistency between modelling and statistical results.

In this study, one major challenge was selecting a BLP. There are mainly two approaches: statistical methods (Mahmood and Jia, 2019) and literature- or evidence-based methods (Wang et al., 2010) to detect a change point and select a BLP. The primary limitation to applying statistical change-point methods, such as the Standard Normal Homogeneity Test and the Worsley Likelihood Ratio Test, was the lack of continuous, homogeneous streamflow records for 1931–2020. For example, only one gauging station (Kerki) contains data spanning this period, and even this record includes missing years. Most other stations have data only up to the mid-1990s and with different starting years (Table 1), making tributary-specific statistical change-point detection unreliable. Therefore, a literature-based method was applied to detect a BLP for the study. The literature indicates that most dams, irrigation canals, and agricultural pumping stations in the basin began in the 1960s (Schlüter et al., 2013;

UNEP, 2011). Therefore, the period before 1950 (i.e., 1931 to 1950) was taken as a BLP in this study, during which human interventions were considered negligible. This single basin-wide BLP was adopted to (i) maintain methodological consistency across the basin, (ii) enable comparative attribution of climate change and human activities among tributaries, and (iii) avoid introducing additional uncertainty associated with tributary-specific change points.

Another significant challenge in the basin is the absence of historical daily climate data for hydrological modelling dating back to 1931. Existing station-based climate data is generally sparse. The only daily meteorological dataset we found covering the period before 1950 is the recently developed gridded dataset from the Climatic Research Unit (CRU) at the University of East Anglia (UEA). This dataset was created by combining the Japanese Reanalysis (JRA) dataset with the CRU TS 4.08 dataset (Harris and UEA-CRU, 2023). It has been applied for the first time in a basin-level hydrological modeling, particularly in the ADRB, where it showed very promising results. Additionally, the dataset was used by Araghi and Martinez (2024) for modeling wheat production systems in Iran and by Yin et al. (2025) for the detection of global compound climate events. Wang et al. (2025) also employed it as one of three meteorological forcing datasets to drive the Canadian Land Surface Scheme Including Biogeochemical Cycles (CLASSIC) model, aiming to assess the influence of topography and meteorological forcing on global snow simulations. To overcome these data limitations and ensure robust results, this study integrated a diverse array of data sources—from local monitoring agencies to global datasets—bringing together multiple scales of information to support a comprehensive assessment.

The core objectives of this study were to quantify the impacts of climate change and human activities for the impacted period (1951–2020) relative to the baseline period (1931–1950) in the Amudarya River Basin, and to examine these impacts on a decadal scale to capture temporal variability in greater detail. In addition, the climate elasticity of streamflow with respect to precipitation, temperature, actual evapotranspiration, and potential evapotranspiration was assessed to identify the most influential climatic drivers of streamflow change. All analyses were conducted using 90 years of hydroclimatic data (1931–2020) at 20 to 30 hydrological and meteorological locations across nearly all major tributaries of the Amudarya, including the Zeravshan and Qashqadarya Rivers, using the hydrological modelling approach and climate elasticity analysis. Several key challenges related to data availability and methodological limitations were successfully addressed in this study, providing a useful reference for future research in the basin. The findings of this study provide a clearer understanding of how climate change and human activities jointly influence streamflow dynamics in the basin.

These insights can support more informed water allocation, reservoir operation, and long-term adaptation planning under increasing climatic and socio-economic pressures.

2 Study area and data

2.1 Study area

The ADRB is a transboundary watershed of significant importance, covering 74% of Tajikistan's area, 13% of Afghanistan, 8.5% of Uzbekistan, 2% of Kyrgyzstan, and 1.7% of Turkmenistan (Mahmood et al., 2025). The majority of streamflow (approximately 80–90%) is generated in the upstream mountainous regions of Tajikistan (75.6%), followed by Afghanistan (14.5%) (Mahmood et al., 2024; SIC-ICWC, 2025). Stretching over 2,540 km, it is Central Asia's largest River (Schlüter et al., 2013). The study area, as shown in Figure 1a, covers 465,000 km^2, including the Zeravshan and Qashqadarya basins. There are about 25 tributaries in the basin (Figure 1a). Among them, the Panj, Vakhsh, Kunduz, Kofirnihon, Surkhandarya, Zeravshan, and Qashqadarya Rivers are the main tributaries of the Amudarya (Wang et al., 2016).

The ADRB can be broadly divided into three main regions: upstream (headwater), midstream, and downstream. The first region lies above the Kerki hydro-station and includes the Pamir-Alay-Hindukush mountain ranges. This region ranges in elevation from 300 m to 7400 m AMSL, with an average of about 3700 m AMSL (Figure 1b). It is characterised by extensive snow and glaciers, contributing approximately 80% to 90% of the river's flow (Schlüter et al., 2013). The second region primarily consists of fertile agricultural land (between Kerki and Kyzyl-jar). In contrast, in the third region, the flow spreads out over the delta (below the Tuyamuyun Hydroelectric Complex near Nukus city) and ultimately reaches the Aral Sea. In the last two regions, elevations range from roughly 28 to 500 m AMSL (Figure 1b), with landscapes comprising huge deserts, patches of grassland, large plains, and arid forests (UNEP, 2011). The ADRB experiences a continental climate with cold winters, hot summers, and limited rainfall. It spans from a tundra climate in the far east to a cold desert climate in the northwest (Salehie et al., 2022b). The basin's annual average temperature is between 11°C and 14°C, with seasonal extremes from -20°C in winter to 35°C in summer. Average annual precipitation is around 464 mm, varying from about 100 mm in the lower reaches to 2000 mm in the eastern Pamir (Salehie et al., 2022a). This precipitation, combined with winter's snow, spring's rain, and summer's ice melt, generates an average annual streamflow of 2470 m^3/s (78 km^3). The recorded maximum and minimum annual streamflows are 3455 m^3/s (109 km^3) and 1838 m^3/s (58 km^3), respectively (UNEP, 2011).

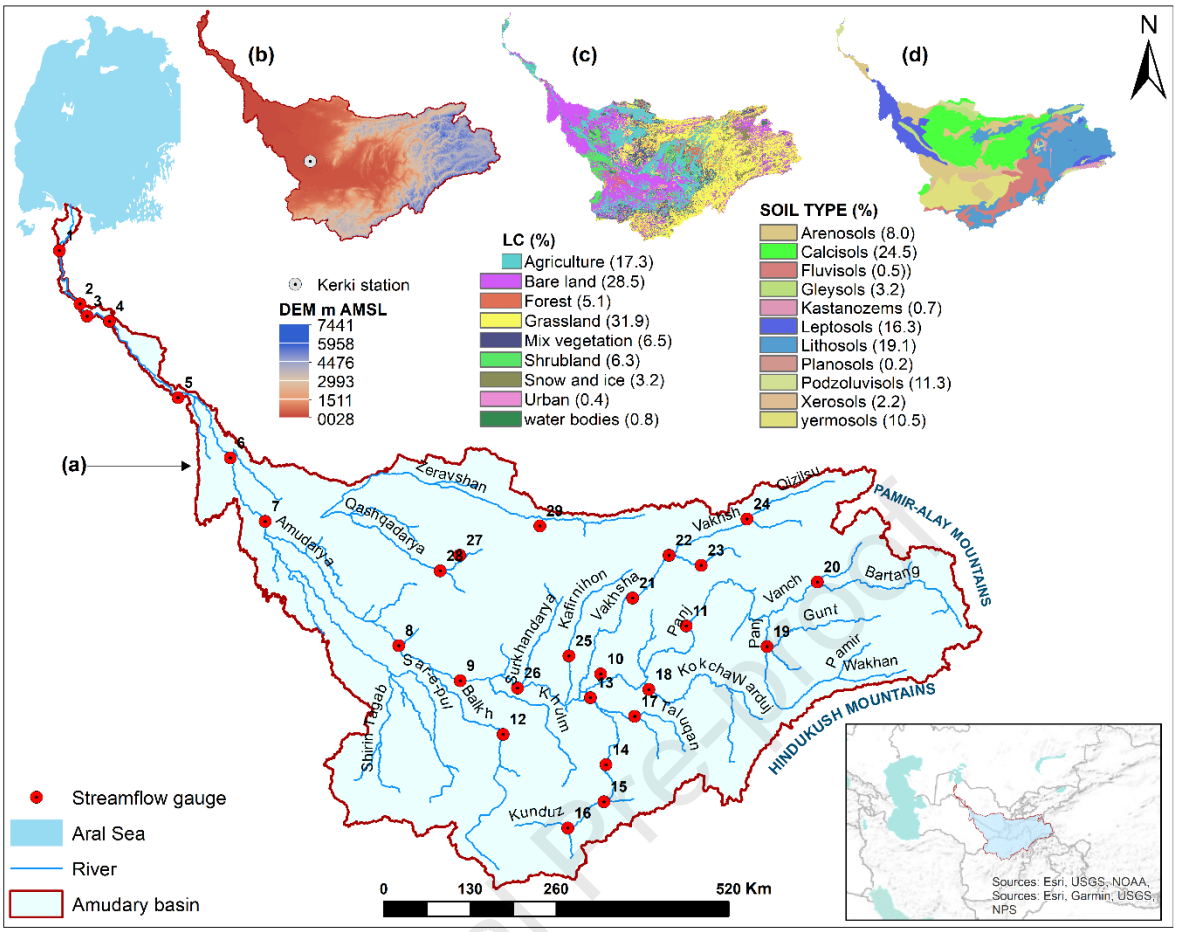

174

175 Figure 1. Geographical location of the Amudarya River basin, showing hydroclimatic data, land-use-land cover,

176 soil types, and elevation in the basin.

177 **2.2 Data description**

178 Streamflow data of the Kerki, Samanbay, Dargan-Ata, Tuyamuyun, Kyzyl-jar, and Kipchak stations, covering the
179 periods 1990–2020 and 1980–1989, was obtained from the Scientific Information Center of the Interstate
180 Commission for Water Coordination (SIC-ICWC) of Central Asia and CaWater (http://www.cawater-info.net/),
181 which are located on the middle and lower reaches of the River (Figure 1a). The primary streamflow data,
182 however, was obtained from the Global Runoff Data Centre (GRDC), a worldwide record founded in 1988 that
183 holds daily and monthly streamflow records from over 10,000 stations (www.bafg.de/GRDC/). All streamflow
184 data between 1931 and 1995 is detailed in Table 1, and their positions are depicted in Figure 1a. Since most GRDC
185 data is limited to the 1980s, additional data from 1982 to 2015 for the Komsomolabad and Tutkaul stations were
186 obtained from Gulakhmadov et al. (2021) and Nikolaevich and Munavvarovich (2019), both sourced from
187 Tajikistan's Ministry of Energy and Water Resources. Streamflow records of Doab, Pull-I-Khomri, and Kulukh
188 Tepa along the Kunduz River were provided by Akhundzadah et al. (2020) from 2009 to 2018, sourced from
189 Afghanistan's Ministry of Energy and Water.

190 Before analysis, streamflow records were screened for missing values and outliers. No infilling was performed
191 for long data gaps; only periods with continuous streamflow observations were used in the analysis. Short gaps
192 (1–3 consecutive missing values) were filled by averaging the preceding and subsequent observations, and the
193 values were also checked against the corresponding precipitation record. Potential outliers were identified by
194 cross-checking streamflow values against precipitation records for the same and preceding days, and only values
195 inconsistent with hydrometeorological conditions were treated as outliers. This approach minimized artificial
196 modification of the observed streamflow signals.

197 Climate data (i.e., precipitation, maximum temperature (Tmax), minimum temperature (Tmin), and relative
198 humidity for 1931–2020 was obtained from the CRU-JRA v2.5. This gridded dataset offers ten key meteorological
199 variables, developed by the CRU at the University of East Anglia. Designed primarily for driving environmental

and hydrological models, this dataset spans 1901 to 2023, which is available at a 0.5° latitude by 0.5° longitude global land grid, excluding Antarctica (Harris and UEA-CRU, 2023). The dataset is regenerated by combining the Japanese Meteorological Agency's JRA reanalysis (JRA-55) data (Kobayashi et al., 2015) and the CRU-TS v4.08 (Harris et al., 2020) to improve consistency with observed climatology, and has been applied in different studies, such as Wang et al. (2025) and Yin et al. (2025)

In addition to the CRU-JRA gridded data, observed station-based daily climate data for precipitation and temperature were also obtained from the Global Historical Climatology Network (GHCN), as described in Table S-2 (Supplementary material) (Menne et al., 2012). Notably, about 85% of regional stations lack data from 1931, which was necessary for this study. Therefore, the GHCN data was primarily used to validate the CRU-JRA data. Potential evapotranspiration (PET) spanning 1931–2020 was obtained from the latest version, CRU-TS v4.08 (Harris et al., 2020), and used to calculate climate elasticity indicators.

The spatial data such as the Harmonized World Soil Database v2.0, having a resolution of 30 arc-seconds (Nachtergaele et al., 2012), the Climate Change Initiative Land Cover product of the European Space Agency, having a resolution of 300 m, and NASA's Shuttle Radar Topography Mission (SRTM)-Digital Elevation Model (DEM), having a resolution of 3 arc-second were used to extract physical characteristics and process parameters of the basin. Glacier distribution data was obtained from the Randolph Glacier Inventory (RGI-Consortium, 2017).

Table 1. Description of hydro-meteorological stations in the Amudarya River basin.

SN	Station	River	Latitude (°N)	Longitude (°E)	Elevation (m AMSL)	GRDC		SIC-ICWC/MEWR/MEW (monthly)
						Monthly	Daily	
1	Kyzyl-jar	Amudarya	43.15	59.14	0062	-	-	1980–2020
2	Samanbay	Amudarya	42.44	59.56	0075	-	-	1980–2020
3	Chatly	Amudarya	42.28	59.70	0072	1931–1973	1940–1950	-
4	Kipchak	Amudarya	42.22	60.11	0078	-	-	1980–2020
5	Tuyamuyun	Amudarya	41.21	61.39	0116	-	-	1980–2020
6	Bir-Ata	Amudarya	40.40	62.34	0155	-	-	1980–2020
7	Ilchik	Amudarya	39.54	62.96	0172	-	-	1980-2020
8	Kerki	Amudarya	37.83	65.25	0241	1931–1989	1952–1989	1980-2020
9	Kelif	Amudarya	37.33	66.28	0259	-	-	1980-2020
10	Nizhniy	Panj/Pyandzh	37.33	68.67	0327	1965–1989	-	-
11	Hirmanjo	Panj/Pyandzh	37.9	70.18	0820	-	-	2000–2016
12	Rabat-I-Bala	Balkh	36.58	66.97	0432	-	1964–1978	-
13	Kulukh Tepa	Kunduz	36.98	68.30	0500	-	1966–1980	2014–2018
14	Pull-I-Khomri	Kunduz	36.10	68.67	0562	-	1968–1978	2009–2018
15	Pul-I-Konda Sang	Kunduz	35.60	68.60	0899	-	1967–1978	-
16	Doab	Kunduz	35.27	67.98	1468	-	1967–1978	2009–2018
17	Pul-I-Chugha	Taluqan	36.73	69.20	0558	-	1960–1978	
18	Khojagar	Kokchah	37.08	69.47	0446	-	1964–1978	2009–2018
19	Khorog	Gunt	37.53	71.52	2070	-	1940–1985	1986–2014
20	Ustie	Kudara	38.33	72.48	2714	1942–1978	-	-
21	Tutkaul	Vakhsh	38.33	69.30	0692	1932–1967	-	1979–2015
22	Komsomolabad	Vakhsh	38.87	69.98	1258	1949–1989	-	1990–2015
23	Tavildara	Vakhsh/Obikhingob	38.70	70.52	1616	1958–1985	-	-
24	Dombrachi	Vakhsh/Qizilsu	39.27	71.38	1841	1961–1985	-	-
25	Tartki	Kofirnihon/Kafirnigan	37.60	68.15	0436	1932–1992	-	-
26	Manguzar	Surxondaryo/Surkhandarya	37.20	67.25	0302	1932–1989	-	-
27	Chirakchi	Qashqadarya	39.03	66.35	0510	1932–1989	-	-
28	Varganza	Qashqadarya	38.83	66.00	0818	1932–1995	-	-
29	Dupuli	Zeravshan	39.38	67.77	1041	1932–1995	-	-

GRDC, *Global Runoff Data Center*, MEWR, *The Ministry of Energy and Water Resources of the Republic of Tajikistan*, MEW, *The Ministry of Energy and Water, Afghanistan*, "-" *data not available*

3 Methodology

Figure 2 describes the overall methodology applied in this study. Firstly, physical characteristics extracted from DEM and the input data, such as precipitation, temperature, and streamflow, were fed into the hydrological model (HEC-HMS) to simulate streamflow. Secondly, the impacts of climate change and human activities were separated using the hydrological approach, and lastly, hydrological responses to climate variables were determined using the climate elasticity method. Each method is described in the following sections:

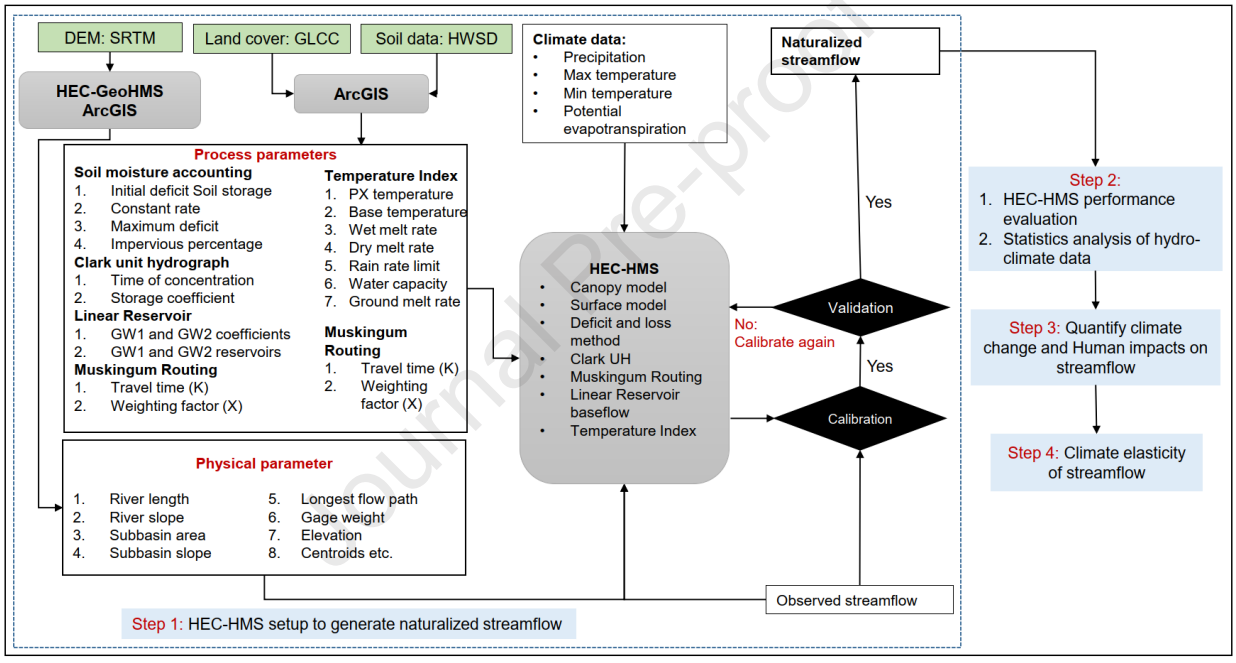

Figure 2. Schematic diagram showing the methodology applied in this study.

3.1 HEC-HMS setup

3.1.1 Model description

The HEC-HMS hydrological model, developed by the US Army Corps of Engineers Hydrologic Engineering Centre (HEC), is a physically based, semi-distributed hydrological tool designed to simulate a wide range of hydrological functions across various watershed systems, ranging from simple to complex streamflow networks

(USACE, 2023). It can generate continuous hydrographs over extended periods or single-storm hydrographs. Due to its reliability, ease of use, data accessibility, and overall accuracy, HEC-HMS was rated top by Keller et al. (2023) among 22 commonly used models. Its versatility makes it suitable for diverse hydrological applications worldwide, such as climate impact assessment, flood forecasting, water supply management, and resource assessment (Mahmood et al., 2020).

This study used the Deficit and Constant Method and the Hamon evapotranspiration method to estimate excess precipitation and evapotranspiration, and simulate continuous hydrological processes. The model also incorporated methods such as the Clark Unit-Hydrograph for hydrograph transformation, the Linear Reservoir Method for baseflow simulation, Lag Routing for channel flow, a Simple Canopy for canopy interception and transpiration, and a Simple Surface Storage for surface storage estimation. Given that snow and ice melt contribute significantly to the region's streamflow (about 75%, as noted by Armstrong et al. (2019), a Temperature Index algorithm for snow/ice melt was integrated into the setup. For this, subbasins are commonly subdivided into 3 to 5 elevation bands to enhance accuracy and capture elevation-dependent variations, as by Mahmood et al. (2019). However, this method does not explicitly simulate snow/glacier mass balance or quantify the individual contribution of snow/glacier melt to total streamflow. Due to the lack of long-term, basin-wide observations of glacier mass balance and snow water equivalent data, an energy-balance or fully distributed glacier model could not be applied. As a result, meltwater contributions are implicitly included in the simulated runoff through the this method, rather than being separately quantified. Consequently, trends in glacier or snow cover were not analysed independently in this study. This limitation may introduce uncertainty in high-elevation catchments and will be addressed in future studies using glacier-specific datasets and physically based melt models.

A crucial part of developing the HEC-HMS involves preparing the initial estimates of the model’s parameters, which are generally divided into physical and process parameters (Kan et al., 2019). Physical parameters—such as subbasin area, slope, and reach length—that define watershed characteristics were derived from SRTM-DEM

(Mahmood and Jia, 2022). Process parameters, such as surface water storage, water infiltration, snow/ice melt rates, and crop coefficients, representing the basin's functional processes and controlling hydrological behaviour (Kan et al., 2019), were estimated using LULC and soil data. These are confirmed during calibration, as they cannot be measured directly due to complexities, knowledge gaps, limitations in measurement methods, data inaccuracy, and a basin's spatial and temporal variability (Garna et al., 2023). Detailed procedures for rational estimation of these parameters can be found in Ahbari et al. (2018) and Mahmood and Jia (2022). The parameters used in calibration are listed in Table S-3 (Supplementary).

3.1.2 Calibration and validation

HEC-HMS was calibrated and validated using 20 streamflow gauges in the region. For 10-13 gauges, 10 years of streamflow were used for calibration and validation, and 4 to 8 years for the remaining gauges, as described in Table 2. Only stations and periods with minimal water extraction were selected for the model calibration to ensure naturalized streamflow for this study. For sites such as Kerki and Chatly, located along the middle and lower reaches of the river, the model calibration focused on the period from 1931 to 1950 because large-scale irrigation and reservoir construction began in the 1960s. Above Kerki (headwater region), we explicitly selected gauges and periods with minimal water withdrawal for the model calibration. For example, the Kulukh-Tepa gauge near the Kunduz River outlet was excluded, as it experienced significant water extraction between the Pull-I-Khomri and Kulukh-Tepa gauges from 1965 to 1978. This careful selection ensures the reliability and accuracy of our calibration process.

Model calibration was conducted using a hybrid approach that combined physically based parameter estimation, automated optimization, and expert-guided manual adjustment. Initial parameter values were derived from land cover, soil, and DEM datasets to ensure physical realism. An automated calibration using the simplex (Nelder-Mead) optimization algorithm, with the Nash–Sutcliffe efficiency (NSE) as the objective function, was then applied to constrain parameter ranges. Additional automated methods, including Univariate and Differential-

Evolution algorithms, were also tested but produced unrealistic parameter values and failed to yield acceptable results (e.g., NSE), particularly in this large and complex basin. Therefore, calibration was finalized manually by adjusting sensitive parameters, including crop coefficient, snow/ice melt rate, loss rate, groundwater coefficient-1 and -2, and groundwater fraction-1 and -2 (Supplementary Material, Table S-4 and Figure S-1), starting with the uppermost streamflow station. These sensitive parameters were reported by Mahmood and Jia (2022) in the ADRB. This approach followed a large-scale hydrological modelling methodology and is consistent with the methodologies detailed in Mahmood and Jia (2022) and Dariane et al. (2016).

Another significant challenge in the model calibration was the limited number of daily streamflow stations. So, the model was also calibrated using monthly streamflow by simulating daily streamflow and converting it to monthly for evaluation against observations. For the performance assessment, we employed NSE, standardized root mean square error (SRMSE), and Percent Volume Deviation (PVD), complemented by graphical presentations, as by Mahmood and Jia (2019) and Wang et al. (2016).

$$NSE = 1 - \frac{\sum(Q_{sim} - Q_{obs})^2}{\sum(Q_{obs} - \overline{Q_{obs}})^2} \quad (1)$$

$$PVD\ (\%) = 100 \times \frac{\sum(Q_{sim} - Q_{obs})}{\sum Q_{obs}} \quad (2)$$

$$SRMSE = \frac{1}{\sigma} \times \sqrt{\left(\frac{1}{n}\sum_{i=1}^{n}(Q_{sim} - Q_{obs})^2\right)} \quad (3)$$

Q_{obs}, Q_{sim}, and σ describe observed streamflow, simulated streamflow, and standard deviation of simulated streamflow, respectively. The PVD and SRMSE values are close to 0, and the NSE values are close to +1.0, indicating good model performance. According to Moriasi et al. (2015), for watershed-scale hydrological models like HEC-HMS, flow simulation performance is considered satisfactory if NSE > 0.50 and PBIAS $\leq \pm 15\%$. Model performance is considered very good if NSE > 0.80. The acceptable value of SRMSE is ≤ 0.5.

3.2 Quantification of climate change and human impacts on streamflow

To date, many methods have been applied for quantifying the impacts of climate variability and human interventions (activities) on streamflow, which are categorized into four main groups: hydrological modelling, conceptual, analytical, and experimental approaches, and are reviewed comprehensively by Dey and Mishra (2017). This study applied the hydrological modelling approach to assess the individual impacts of CC and HA on the streamflow. It is the most common way to explore the impact of climate change and anthropogenic activities on streamflow (Li et al., 2020). However, more information is required to calibrate a hydrological model and long-term time series to determine the BLP (Mahmood and Jia, 2019).

There are two main steps of this approach. The first step is to determine the BLP, the period when human interventions (e.g., dams, canals, deforestation, and urbanization) can be considered negligible. It can be explored through change-point analysis or through the literature-based method. In this study, we selected the period 1931–1950 as a BLP using a literature-based approach, and more details on the BLP selection are provided in the introduction section. Therefore, the entire study period (1931–2020) was divided into the BLP (1931–1950) and the impacted (altered) period (1951–2020).

The second step is to calibrate a hydrological model for the BLP and simulate naturalized streamflow for the impacted period (IPP) using only climate data, without considering human interventions (Hu et al., 2015). The simulated naturalized streamflow can be referred to as the hydrological response solely to changing climate variability, whereas the measured (observed) streamflow is the hydrological response to the combined effects of climate change and human activities (Hu et al., 2015; Mahmood and Jia, 2019). After dividing the observed streamflow and naturalized streamflow for the BLP and IPP, changes in streamflow due to climate change and human activities can be separated and quantified as below (Hu et al., 2015; Wang et al., 2013):

$$\Delta Q_T(\%) = \Delta Q_C + \Delta Q_H = 100 \times (Q_{OI} - Q_{OB})/Q_{OB} \quad (4)$$

$$\Delta Q_C(\%) = 100 \times (Q_{SI} - Q_{SB})/Q_{SB} \quad (5)$$

$$\Delta Q_H(\%) = \Delta Q_T - \Delta Q_C \quad (6)$$

Equation 4 calculates the total relative change in streamflow (ΔQ_T) in the IPP (1951–2020) relative to the BLP (1931–1950). Here, Q_{OI} is the observed streamflow during the impacted period (with both climate change and human activities), and Q_{OB} is the observed streamflow during the BLP. The formula expresses the total change as a percentage of the baseline streamflow. This total change results from the combined effects of both climate change and human activities. Equation 5 quantifies the relative change in streamflow due to climate change (ΔQ_C) alone. It compares simulated natural streamflow under current climate conditions (Q_{SI}) with simulated streamflow under baseline climate conditions (Q_{SB}), assuming no human influence. This separates the impact of climate variability on streamflow, expressed as a percentage relative to the baseline. Equation 6 segregates the relative contribution of human activities to streamflow change (ΔQ_H). It is calculated by subtracting the climate-induced change (ΔQ_C) from the total observed change (ΔQ_T). This approach assumes that the effects of climate change and human activities on streamflow are additive and separable. In short, these equations provide a framework to distinguish and quantify the individual impacts of climate change and human activities on river streamflow dynamics, which is crucial for understanding hydrological changes and for planning adaptive water management strategies. In some studies, such as (Dey and Mishra, 2017; Hu et al., 2015; Wang et al., 2008; Wang et al., 2013), ΔQ_C has been calculated as:

$$\Delta Q_C(\%) = 100 * (Q_{SI} - Q_{OB})/Q_{OB} \quad (7)$$

However, we used equation 5 as in Mahmood and Jia (2019) because there are always some biases between simulated streamflow and observed streamflow, and a hydrological model cannot capture all the variation of observed streamflow. This can mislead the original changes due to climate change and human activities. The contributions of ΔQ_C and ΔQ_H to total change in streamflow (ΔQ_T) are calculated as below:

$$P_C(\%) = \frac{\Delta Q_C}{\Delta Q_T} \times 100 \text{ and } P_H(\%) = \frac{\Delta Q_H}{\Delta Q_T} \times 100 \quad (8)$$

343 P_C (%) and P_H (%) represent the percentage contribution of climate change and human activities to the total
344 streamflow change. These equations help quantify how much of the observed streamflow change is due to climate
345 variability and how much is due to human-induced factors like land use change, water withdrawal, or reservoir
346 operations. This separation is crucial for understanding the dominant drivers of hydrological change and for
347 designing appropriate water management and adaptation strategies. Finally, the overall (1951–2020) and decadal
348 changes in streamflow due to climate variability, human activities, and both factors (climate and human) were
349 estimated in all the main tributaries in the basin. Additionally, changes in climatic variables (i.e., precipitation,
350 Tmax, Tmin, and Tmean) were assessed at the decadal scale to examine climatic variability in the IPP relative to
351 the BLP and identify plausible drivers of streamflow changes in the region.

352 **3.3 Climate elasticity**

353 Climate elasticity is key in projecting the hydrological response to climate change or climate variables. At the
354 watershed level, the climate elasticity of hydrological variables (e.g., streamflow) is considered a vital indicator
355 of the sensitivity of streamflow to a changing climate (Yang and Yang, 2011). This study applied hydrological
356 modelling and statistical methods to examine the climate elasticity of streamflow with respect to temperature,
357 precipitation, actual evapotranspiration (AET), and PET. In the modelling approach, the calibrated HEC-HMS
358 model was forced with a 10% increase in precipitation, evapotranspiration, and temperature, and the resulting
359 streamflow simulations were compared with the baseline simulations to assess the climate elasticity of streamflow.
360 Similar climate perturbation ranges (±10–25%) have been adopted in previous elasticity studies mentioned in
361 Sankarasubramanian et al. (2001). In the statistical approach, two mostly used non-parametric indicators
362 developed by Sankarasubramanian et al. (2001) and Zheng et al. (2009) were applied to estimate the climate
363 elasticity (a dimensionless indicator) of streamflow at 34 sites in the ADRB, which are described below,
364 respectively:

365 $$E_x = median\left(\frac{(Q_i-\overline{Q})/\overline{Q}}{(X_i-\overline{X})/\overline{X}}\right) \quad (9)$$

$$E_x = \frac{\overline{X}}{\overline{Q}} \times \left(\frac{\sum(X_i-\overline{X})\times(Q_i-\overline{Q})}{\sum(X_i-\overline{X})^2}\right) = R_{X.Q} \times \frac{CV_Q}{CV_X} \quad (10)$$

Where E_x is the climate elasticity of streamflow (Q) with respect to precipitation or PET (X). Xi and Qi are annual precipitation/PET and annual streamflow time series, while $\overline{X}$ and $\overline{Q}$ are the long-term averages of climate variables and streamflow, respectively. $R_{X.Q}$, CV_Q, and CV_X are the correlation coefficients between Q and X, the coefficient of variation of Q, and the coefficient of variation of X, respectively. Zheng's formula indicates that the higher the $R_{X.Q}$ and CV_Q /CV_X values, the more vulnerable or sensitive the streamflow is to the climate variable. These indicators were estimated using annual time series of precipitation and PET from CRU, and simulated streamflow data from HEC-HMS for 1931–2020.

4 Results

4.1 Calibration and validation

Table 2 describes the NSE, PVD, and SRMSE indicators used to evaluate the model. On average, NSE values were 0.73 (0.56–0.92) during calibration and 0.74 (0.53–0.93) during validation. PVD values ranged from -21% to 30%, averaging 4.08% during calibration and 3.69% during validation, while SRMSE values varied between 0.26 and 1.19, with averages of 0.58 and 0.62 for calibration and validation, respectively, across the basin's hydro-stations. The evaluation indicated acceptable results, with high NSE and low PVD/SRMSE at all main stations, including Chatly, Kerki, Nizhny, and Tutkaul. However, performance was comparatively lower at higher-elevation stations, particularly those on the Afghanistan side (e.g., Rabat-I-Bala, Baghlan, Doab, and Khojagar). This discrepancy may be due to lower-quality hydroclimatic measurements, as maintaining gauges in mountainous regions with heavy snowfall and glacial contributions is challenging.

Furthermore, accurately modelling hydrological processes in glacierized basins requires detailed data on glacier mass balance and snow cover. However, such data are often scarce, increasing uncertainty in model outputs. For instance, Schaefli and Huss (2011) noted that limited seasonal mass-balance data can hinder the calibration of hydrological models in high-mountain catchments. Similarly, Finger et al. (2011) emphasized that the lack of

389 comprehensive glacier mass-balance and snow-cover observations can reduce the performance of physically based
390 hydrological models. Additionally, measuring precipitation accurately in high-altitude regions is complex due to
391 sublimation and blowing snow (Tobias Siegfried, 2024). Since streamflow measurement typically relies on the
392 stage-discharge method, errors can arise from various factors, including measurement inaccuracies in river stage
393 and discharge, errors in rating curve parameterization, interpolation and extrapolation errors, unsteady flow
394 conditions, and seasonal vegetation changes (Di Baldassarre and Montanari, 2009).
395 Figure 3 shows that the simulated streamflow closely matched the observed streamflow components, including
396 low flows, rising limbs, and falling limbs, though it struggled with peak flows in some years. These differences
397 are likely due to the previously mentioned climate, streamflow, and HEC-HMS-related limitations.

Table 2. Performance evaluation of the hydrological model at different hydro-stations in the Amudarya River basin for 1931–2020.

SN	Station	River	Calibration			Validation			Period	
			NSE	PVD (%)	SRMSE	NSE	PVD (%)	SRMSE	Calibration	Validation
1	Chatly	Amudarya	0.89	-1.37	0.379	0.93	-0.14	0.26	1931–1940	1941–1950
2	Kerki	Amudarya	0.87	7.50	0.382	0.91	-1.26	0.30	1931–1940	1941–1945
3	Rabat-I-Bala	Balkh	0.59	3.13	0.676	0.86	3.35	1.03	1964–1971	1972–1976
4	Khorog	Gunt	0.74	4.60	0.498	0.79	16.78	0.46	1940–1949	1950–1959
5	Tartki	Kofirnihon/Kafirnigan	0.72	-11.83	0.782	0.87	-14.63	0.48	1932–1941	1942–1951
6	Khojagar	Kokchah	0.47	6.89	0.661	0.88	4.54	0.58	1965–1970	1971–1976
7	Ustie	Kudara	0.69	1.37	0.614	0.57	-21.32	0.76	1951–1960	1965–1970
8	Pul-I-Konda Sang	Kunduz	0.85	8.34	0.529	0.70	12.92	0.61	1969–1975	1975–1979
9	Pull-I-Khomri	Kunduz	0.56	-10.09	1.087	0.56	-8.01	1.19	1968–1973	1974–1977
10	Doab	Kunduz	0.66	10.01	0.628	0.92	22.85	0.58	1969–1975	
11	Nizhny	Panj/Pyandzh	0.82	-3.18	0.46	0.78	5.73	0.548	1970–1979	1980–1989
12	Manguzar	Surxondaryo/Surkhandarya	0.75	6.90	0.507	0.60	8.18	0.68	1933–1942	1943–1952
13	Pul-I-Chugha	Taluqan	0.71	-3.94	0.724	0.54	9.37	0.84	1968–1973	1974–1977
14	Tutkaul	Vakhsh	0.91	03.32	0.347	0.81	-10.91	0.51	1932–1941	1942–1951
15	Komsomolabad	Vakhsh	0.92	0.70	0.327	0.84	13.55	0.43	1951–1957	1977–1986
16	Tavildara	Vakhsh/Obikhingob	0.72	29.34	0.510	0.65	29.41	0.54	1959–1968	1969–1978
17	Dombrachi	Vakhsh/Qizilsu	0.72	20.20	0.531	0.79	9.18	0.62	1961–1970	1971–1980
18	Chirakchi	Qashqadarya	0.70	1.33	0.54				1932–1936	1937–1940
19	Varganza	Qashqadarya	0.71	-1.72	0.59	0.58	-0.36	0.75	1931–1940	1941–1950
20	Dupuli	Zeravshan	0.77	9.36	0.51	0.75	-6.11	0.63	1932–1941	1942–1951
		Average	0.73	4.08	0.58	0.75	3.69	0.62		

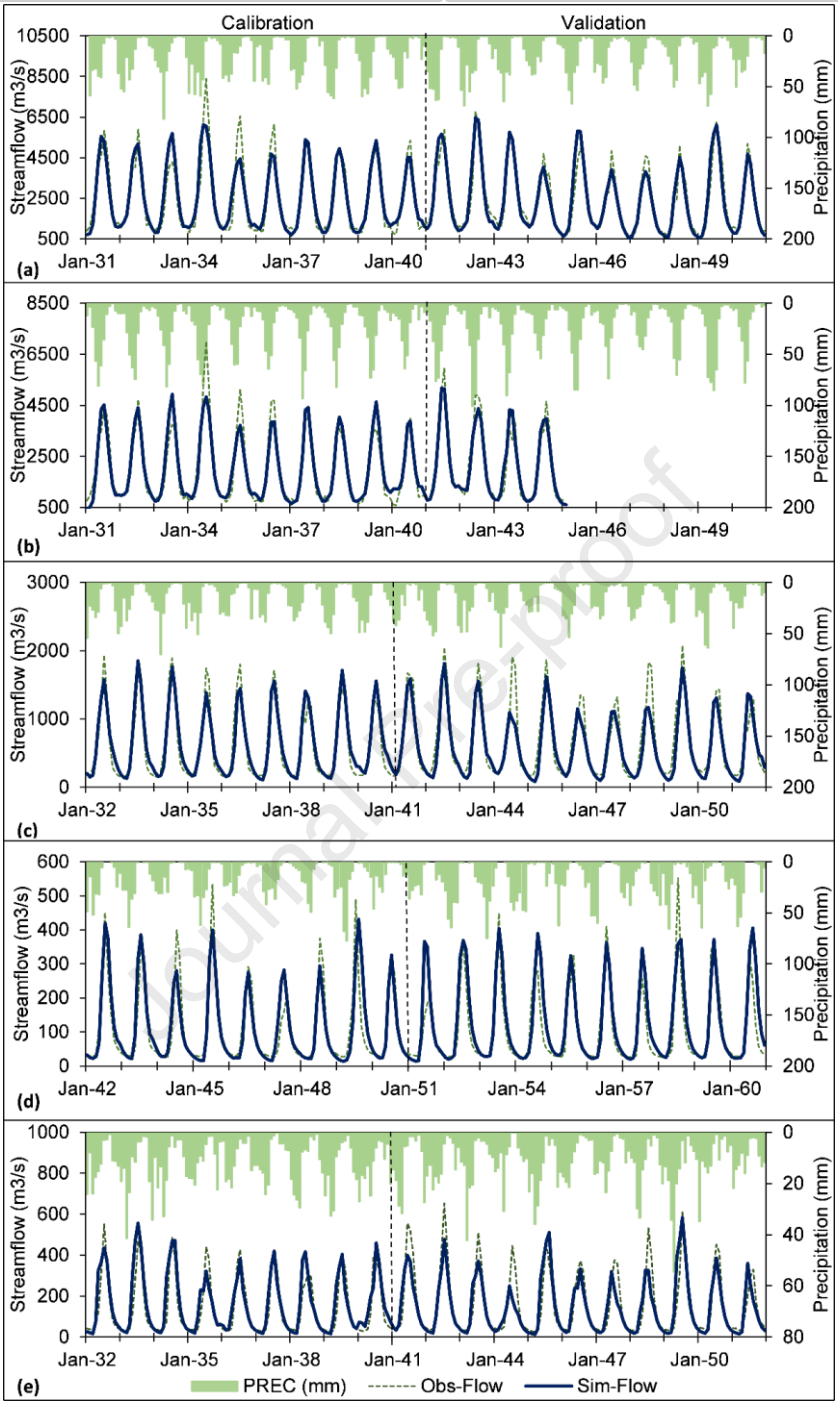

401

402 Figure 3. Model evaluation at the main hydro stations located in the Amudarya basin: a) Chatly, b) Kerki, c)

403 Tutkaul, d) Khojagar, e) Dupuli.

4.2 Mean annual statistics

Table 3 summarizes the mean annual hydroclimatic statistics for the ADR's main tributaries—Panj, Vakhsh, and Kunduz Rivers—using CRU-JRA climate data, observed (for available period), and simulated naturalized streamflow from 1931 to 2020. To compute these climate averages, we used an arithmetic mean across all grid cells within the whole basin and its sub-basins, since CRU-JRA provides spatially gridded data. For temporal aggregation of climate and streamflow data, annual means were first calculated for each variable, and the long-term values reported in Table 3 were obtained by averaging these annual means over the full period (1931–2020). Basin-wide average Tmax, Tmin, and Tmean were 17.26°C, 4.45°C, and 10.87°C, respectively, with notable spatial variation. Precipitation ranged from 220 mm (Gunt) to 787 mm (Kunduz), averaging 394 mm basin-wide. The Amudarya's naturalized mean annual flow was 2618 m^3/s (82.6 km^3/yr), compared to 2470–2540 m^3/s (78–80 km^3/yr) in literature (UNEP, 2011).

The Panj and Vakhsh accounted for 66% of the total flow, while the other tributaries contributed 2–8%. The observed flow at Kyzyl-jar has been reduced by 83% relative to naturalized flow, with greater reductions in the middle and lower reaches. The headwater above Kerki contributed 82% of the total flow. Additional hydroclimatic statistics for the BLP and IPP regions are presented in Table S-5 (Supplementary), indicating notable increases in temperature and precipitation and mostly reduced streamflow.

421 Table 3. Mean annual statistics of all the main rivers at 25 streamflow gauges in the Amudarya River basin.

SR	River	Station	Tmax (°C)	Tmin (°C)	Tmean (°C)	P_{RECIP} (mm)	NS-flow m^3/s	OS-flow m^3/s
1	Amudarya	Kyzyl-jar	17.26	4.47	10.87	394	2618	435
2	Amudarya	Chatly	17.26	4.47	10.87	394	2618	1412
3	Amudarya	Tuyamuyun	17.25	4.46	10.86	396	2606	832
4	Amudarya	Bir-Ata	17.2	4.43	10.82	396	2561	1106
5	Amudarya	Kerki	17.04	4.15	10.59	364	2149	1578
6	Amudarya	Kelif	17.04	4.15	10.59	364	2149	1876
7	Panj	Nizhny	21.07	7.72	14.4	264	1016	1006
8	Panj	Hirmanjo	20.28	7.07	13.67	270	686	809
9	Balkh	Rabat-e-Bala	7.03	-3.96	1.54	746	50	50
10	Kunduz	Kulukh Tepa	15.76	2.81	9.28	306	163	102
11	Kunduz	Pull-I-Khomri	10.43	-1.71	4.36	417	68	71
12	Kunduz	Pull-I-Konda Sang	4.49	-6.95	-1.23	550	37	31
13	Kunduz	Doab	0.31	-10.65	-5.17	787	8	9
14	Taluqan / Kunduz	Pull-I-Chugha	22.36	8.44	15.4	263	70	65
15	Kunduz	Chardara	13.36	1.1	7.23	459	87	54
16	Kokchah / Panj	Khojagar	22.76	9.37	16.06	274	218	196
17	Gunt / Panj	Khorog	22.15	9.19	15.67	220	123	104
18	Bartang / Panj	Ustie	15.29	1.69	8.49	387	29	35
19	Vakhsh	Tutkaul	21.59	8.3	14.95	418	683	635
20	Vakhsh	Komsomolabad	21.22	8.02	14.62	427	683	632
21	Vakhsh	Garam	21.22	8.02	14.62	427	446	316
22	Kofirnihon	Tartki	22.24	8.46	15.35	316	147	164
23	Surkhandarya	Manguzar	13.52	0.82	7.17	296	68	54
24	Qashqadarya	Chirakchi	5.33	-5.81	-0.24	552	36	22
25	Zeravshan	Dupuli	11.52	-0.45	5.53	457	209	154

422 Tmax, *maximum temperature*, Tmin *minimum temperature*, Tmean *mean temperature*, Prec *precipitation*, NS-flow *naturalized mean annual streamflow*,

423 OS-flow *observed mean annual streamflow*,

424

4.3 Impacts of climate change and human activities

4.3.1 Climatic variability

Figure 4 (columns 2–5) shows the changes in precipitation, Tmax, Tmin, and Tmean, and changes in streamflow (columns 6–8) due to climate change, human activities, and the combined effect of both factors. More detail is provided in Table S-6 (Supplementary Materials). In the entire basin (above Kyzaljar), Tmax, Tmin, and Tmean increased in all decades except Tmax in the 1950s relative to the BLP, with an overall increase of 0.45°C, 0.88°C, and 0.67°C, respectively. The maximum increases in Tmax and Tmean were observed in the 2000s (1.13 °C and 1.41 °C, respectively), and in Tmin, it was observed in the 2010s (1.74 °C). The basin also showed an overall increase in precipitation of 9.8%, with a minimum in the 1970s and a maximum in the 2010s (Figure 4a). Similar climatic changes were observed at the Tuyamuyun and Bir-Ata sites (Figure 4 (b–c)). However, the temperature and precipitation increases in the headwater region (above Kekri) were slightly higher than in the whole basin (Figure 4 d and e). In the Balkh and Kunduz basins, an increase in Tmax, Tmin, Tmean, and precipitation ranged from 0.23–0.59 °C, 0.79–1.10 °C, 0.51–0.81°C, and 8.4–13.3%, respectively, at different sites (Figure 4 (f–J)). The Kunduz basin showed a slightly higher increase, specifically in Tmin and precipitation, whereas the Balkh basin showed a slightly lower increase than the whole basin. In the Panj (Amudarya above Nizhny), Vakhsh, Kofirnihon, Surkhandarya, Zeravshan, and Qashqadarya basins, temperature changes were quite similar across the basins and to the whole basin. However, precipitation increases in the Panj, Vakhsh, and Kofirnihon (5.7–8.6%) were lower than the changes in the whole basin, while slightly high values (9.8–12.0%) were observed in the Surkhandarya, Zeravshan, and Qashqadarya basins. Across the ADRB, the maximum increases in Tmax, Tmin, Tmean, and precipitation were observed in Surkhandarya (0.68 °C), Kunduz (1.1 °C), Surkhandarya (0.83 °C), and Kunduz (13%), respectively. The last two decades showed higher increases in climate variables than the average across the whole basin. It was also observed that Tmin has been increasing at a much faster rate than Tmax in the basin. Hu et al. (2021) and Murodov et al. (2023) also showed increases in temperature and

precipitation using trend analysis. It was also observed that climatic variables, especially temperatures, showed a dramatic, continuous increase from the 1980s onward.

4.3.2 Streamflow changes

At Kyzyl-jar (outlet of the ADR) (Figure 4a), streamflow was reduced by 77% during the whole IPP relative to the BLP, out of which CC and HA accounted for 11% and -88%, respectively. This means HA caused a 114% decrease in total streamflow (77% reduction), while CC resulted in a 14% increase in streamflow. A continuous decrease was observed from the 1950s (-27%) to the 2010s (-97%) relative to the BLP. By 1970, more than half of the streamflow had been reduced by HA, and by 1990, more than 90%. The main reason was an immense expansion (150%) in irrigated agriculture during 1950–1990 by the Soviet Union in the ADRB (UNEP, 2011). Across all decades, 3–15% changes in streamflow were estimated due to CC, which contributed about a 4–38% increase; in contrast, HA caused a reduction of 37–112%, contributing about 104–138% to the total. At Chatly/Samanbay, the results were similar to those at Kyzyl-jar because the two sites are very close (Table S-5). At Tuyamuyun and Bir-Ata, streamflow reductions were estimated at 65% and 54%, respectively, attributed mainly to HA (Figure 4 (b–c).

The headwater region (above Kerki, Figure 4d) also showed a 22% reduction in streamflow. The attribution analysis showed that HA accounted for 140% of this reduction. This occurs because CC actually produced a 10% increase in streamflow relative to the BLP (i.e., a +45% contribution). In other words, climate change alone would have increased streamflow, but human activities more than offset this increase, causing the overall decline. Therefore, HA contributions exceeding 100% indicate that human-driven reductions not only counterbalanced the climate-induced gains but also resulted in an additional net decrease in streamflow. The magnitude of reduction at this point is much lower than at Kyzyl-jar. This means the most human activities (e.g., water extraction) occurred between the outlet and Kerki. According to the World-Bank (2004) and UNEP (2011), the network of irrigation canals reached deep into the deserts of Turkmenistan and Uzbekistan. It supplied water to 7.6 million

hectares of agricultural land in 1980. All decades showed a decrease in streamflow, except the 1950s, when CC increased streamflow by 9% but had no HA impact on streamflow. Similar results were observed at Kelif (Figure 4e), but the streamflow reduction (6%) was much lower than at Kerki, even though the sites are very close. This is mainly because of the largest irrigation canal, the Karakum Darya, which diverts about 15% of the flow of the Amudarya near Kerki (Brite, 2018).

In the Kunduz basin, one of the major tributaries of the Amudarya from the southern side, CC and HA were quantified at five sites, where four, i.e., Kulukh Tepa (near outlet), Pull-I-Khomri / Pull-I-Konda Sang (middle), and Doab (upper) are located on the main Kunduz River, and Pull-I-Chugha on the Taluqan River (a tributary of the Kunduz River) (Figure 4 (f–h). At the Doab station, streamflow increased by 88%, with 34% attributed to CC and 54% to HA. These rises are likely linked to reductions in rainfed agriculture, vegetation/grassland, and glacier area. Akhundzadah et al. (2020) showed that between 1992 and 2019, rainfed agriculture, vegetation/grassland, and glaciers, which were 16%, 60%, and 2.5% in 1992, declined by about 30%, 20%, and 33%, respectively. According to Coe et al. (2011) and Levy et al. (2018), deforestation alters the hydrological, geomorphological, and biochemical processes of rivers by reducing evapotranspiration on the land surface and increasing runoff, river discharge, erosion, and sediment fluxes from the land surface. At Pull-I-Khomri, a 21% increase in streamflow was estimated, of which 23% was attributed to CC and -2% to HA during the whole IPP. In contrast, streamflow was estimated to decrease by 30% at Kulukh Tepa, 46% due to HA, and 16% due to CC. The reduction is mainly due to water withdrawal for irrigation by about 19 irrigation canals below Pull-I-Khomri, where the Kunduz River flows through the wide, lowlands of Baghlan and Kunduz provinces, a highly populated area in the basin (Akhundzadah et al., 2020; Varzi and Wegerich, 2008). At Pull-I-Chugha on the Taluqan River, in contrast to Kulukh-Tepa, an increase of 1.7% in streamflow was estimated, where a 13% increase was estimated due to CC and an 11.3% decrease due to HA.

493 The Amudarya above Nizhny is referred to as the Panj (Pyandzh), which is fed by many tributaries, including the
494 Wakhan, Pamir, Gunt, Kokchah, and Bartang (Figure 4). In the Kokchah and Gunt River basins, HA dominated,
495 causing a decrease in streamflow by 1.9% and 10%, respectively (Figure 4i). In contrast, 25% and 5.6% increases
496 in streamflow were calculated at Hirmanjo and Nizhny, respectively (Figure 4(j–k)). Hirmanjo is the second site,
497 where both HA (72%) and CC (28%) contributed positively (increase) to streamflow. At Nizhny, HA also caused
498 an increase in streamflow in the 1960s and 1970s, but a decrease during the entire IPP. The main reasons can be
499 deforestation, as mentioned by Coe et al. (2011), and increased glacier melt in the region, as we observed a positive
500 temperature elasticity of streamflow ranging from 0.51 to 1.04 (section 4.4). In all previous results, we found
501 positive values of CC, but at Khorog in the 1970s and 1980s and Hirmanjo in the 1970s, it was found that CC
502 caused a decrease in streamflow. This was mainly due to decreased precipitation (l and n).
503 In the Vakhsh River basin, the second-largest contributor to the Amudarya, the analysis was performed at the
504 Garam (upper), Komsomolabad (middle), and Tutkaul (middle-lower) stations. At Garam, streamflow was
505 increased by about 3% (8% by CC and -5% by HA), and it decreased by 1.8% (8% by CC and -11% by HA) at
506 Komsomolabad and 2.6% (8% by CC and -10% by HA) at Tutkaul. It was observed that the HA factor increased
507 from Garam (-5%) to Tutkaul (-11%) while the CC factor remained the same (8%). Among all stations, Kyzyl-
508 jar exhibited the strongest human-activity (HA) influence on streamflow change (−114%), whereas Doab showed
509 the largest climate-change (CC) contribution (38%) to streamflow. The results of all 25-gauges in the basin are
510 described in Table S-6 (Supplementary Materials).

Kyzyljar	ΔTx (°C)	ΔTn (°C)	ΔTmn (°C)	ΔP (%)	ΔQ_T (%)	ΔQ_C (%)	ΔQ_H (%)
1950s	-0.10	0.12	0.01	12.3	-27	10	-37
1960s	0.14	0.37	0.26	9.6	-57	10	-67
1970s	0.08	0.44	0.26	1.5	-81	3	-84
1980s	0.51	0.92	0.72	6.4	-93	7	-100
1990s	0.46	0.90	0.68	13.4	-87	17	-104
2000s	1.13	1.68	1.41	12.1	-94	15	-109
2010s	0.93	1.74	1.34	13.5	-97	15	-112
Mean	0.45	0.88	0.67	9.8	-77	11	-88

Manguz-ar	ΔTx (°C)	ΔTn (°C)	ΔTmn (°C)	ΔP (%)	ΔQ_T (%)	ΔQ_C (%)	ΔQ_H (%)
1950s	-0.11	0.12	0.00	11.3	1.0	21	-20
1960s	0.35	0.49	0.42	9.6	-28	20	-48
1970s	0.28	0.56	0.42	4.5	-79	-1.3	-77
1980s	0.70	0.90	0.80	11.0		11	
1990s	0.81	1.04	0.93	11.4		22	
2000s	1.44	1.89	1.66	21.2		35	
2010s	1.30	1.87	1.58	15.1		20	
Mean	0.68	0.98	0.83	12.0	-34	18	-52

Dupuli	ΔTx (°C)	ΔTn (°C)	ΔTmn (°C)	ΔP (%)	ΔQ_T (%)	ΔQ_C (%)	ΔQ_H (%)
1950s	-0.13	0.13	0.00	12.2	0.4	8	-8
1960s	0.20	0.41	0.31	10.4	-1.2	11	-12
1970s	0.18	0.56	0.37	2.2	-0.3	11	-12
1980s	0.59	0.88	0.73	10.4	-4.7	20	-25
1990s	0.61	0.91	0.76	10.1	-2.6	27	-30
2000s	1.22	1.82	1.52	13.3		37	
2010s	1.01	1.73	1.37	10.2		32	
Mean	0.53	0.92	0.72	9.8	-1.6	21	-23

Tartki	ΔTx (°C)	ΔTn (°C)	ΔTmn (°C)	ΔP (%)	ΔQ_T (%)	ΔQ_C (%)	ΔQ_H (%)
1950s	-0.08	0.14	0.03	4.1	3.4	4.3	-1
1960s	0.30	0.48	0.39	6.0	-2.2	2.2	-4
1970s	0.12	0.36	0.24	7.1	-13	3.9	-17
1980s	0.66	0.97	0.81	9.7	-3.9	4.9	-9
1990s	0.83	1.16	0.99	9.0		7.4	
2000s	1.46	1.82	1.64	9.3		14	
2010s	1.25	1.90	1.57	13.9		8.9	
Mean	0.65	0.98	0.81	8.4	-4.0	6.5	-7.8

Tutkaul	ΔTx (°C)	ΔTn (°C)	ΔTmn (°C)	ΔP (%)	ΔQ_T (%)	ΔQ_C (%)	ΔQ_H (%)
1950s	-0.08	0.12	0.02	5.2	0.9	5	-4
1960s	0.22	0.40	0.31	4.3	-4.0	4	-8
1970s	0.08	0.36	0.22	-1.2	-8.2	2	-10
1980s	0.58	0.96	0.77	6.5	-9.9	6	-16
1990s	0.59	0.98	0.78	14.6	-1.4	16	-18
2000s	1.26	1.69	1.47	8.7	1.1	14	-13
2010s	1.05	1.79	1.42	12.3	3.4	12	-8
Mean	0.53	0.90	0.71	7.2	-2.6	8	-11

Tuyamu-yun	ΔTx (°C)	ΔTn (°C)	ΔTmn (°C)	ΔP (%)	ΔQ_T (%)	ΔQ_C (%)	ΔQ_H (%)
1950s	-0.10	0.12	0.01	12.3		10	
1960s	0.14	0.37	0.26	9.6		10	
1970s	0.08	0.44	0.26	1.6		3	
1980s	0.51	0.92	0.72	6.5	-63	7	-70
1990s	0.46	0.90	0.68	13.4	-57	17	-74
2000s	1.13	1.69	1.41	12.2	-69	15	-84
2010s	0.93	1.75	1.34	13.4	-73	15	-88
Mean	0.45	0.88	0.67	9.9	-65	11	-76

Komoso-mulabad	ΔTx (°C)	ΔTn (°C)	ΔTmn (°C)	ΔP (%)	ΔQ_T (%)	ΔQ_C (%)	ΔQ_H (%)
1950s	-0.08	0.10	0.01	5.4	-0.9	5	-5
1960s	0.20	0.37	0.29	4.2	-2.6	4	-7
1970s	0.09	0.35	0.22	-2.8	-4.5	2	-6
1980s	0.59	0.94	0.76	5.2	-8.9	6	-15
1990s	0.56	0.91	0.74	14.5	-0.1	16	-17
2000s	1.23	1.63	1.43	8.8	2.5	14	-12
2010s	1.02	1.73	1.38	11.7	2.2	12	-10
Mean	0.52	0.86	0.69	6.7	-1.8	8	-10

Bir-Ata	ΔTx (°C)	ΔTn (°C)	ΔTmn (°C)	ΔP (%)	ΔQ_T (%)	ΔQ_C (%)	ΔQ_H (%)
1950s	-0.10	0.12	0.01	12.3		10	
1960s	0.15	0.38	0.26	9.6		10	
1970s	0.08	0.44	0.26	1.8		3	
1980s	0.52	0.92	0.72	6.9	-57	7	-64
1990s	0.47	0.91	0.69	13.5	-43	16	-60
2000s	1.14	1.70	1.42	12.3	-54	15	-69
2010s	0.94	1.75	1.34	13.3	-61	15	-75
Mean	0.45	0.89	0.67	10.0	-54	11	-65

Hirmanjo	ΔTx (°C)	ΔTn (°C)	ΔTmn (°C)	ΔP (%)	ΔQ_T (%)	ΔQ_C (%)	ΔQ_H (%)
1950s	-0.08	0.14	0.03	8.0		9	
1960s	0.15	0.39	0.27	5.3		9	
1970s	0.04	0.40	0.22	-2.9	25	-2	
1980s	0.50	0.98	0.74	-0.3	24	1	
1990s	0.47	0.99	0.73	12.3	33	13	20
2000s	1.14	1.69	1.41	6.9	27	10	17
2010s	0.90	1.79	1.35	10.8	22	13	9
Mean	0.45	0.91	0.68	5.7	25	7	18

Kerki	ΔTx (°C)	ΔTn (°C)	ΔTmn (°C)	ΔP (%)	ΔQ_T (%)	ΔQ_C (%)	ΔQ_H (%)
1950s	-0.10	0.14	0.02	11.9	9	9	0.0
1960s	0.20	0.42	0.31	8.5	-9	8	-17
1970s	0.11	0.47	0.29	2.2	-26	2	-28
1980s	0.56	0.95	0.75	8.3	-35	6	-41
1990s	0.57	1.00	0.78	13.1	-21	15	-36
2000s	1.23	1.78	1.51	14.1	-32	14	-47
2010s	1.04	1.84	1.44	12.8	-37	13	-50
Mean	0.51	0.94	0.73	10.1	-22	10	-31

Nizhny	ΔTx (°C)	ΔTn (°C)	ΔTmn (°C)	ΔP (%)	ΔQ_T (%)	ΔQ_C (%)	ΔQ_H (%)
1950s	-0.09	0.14	0.03	8.5		9	
1960s	0.17	0.40	0.29	4.9	20	10	10
1970s	0.04	0.39	0.22	-0.9	14	0	14
1980s	0.51	0.98	0.75	1.3	-4.9	4	-9
1990s	0.51	1.02	0.76	11.6	-1.2	14	-16
2000s	1.18	1.71	1.45	8.1	3.3	11	-7
2010s	0.96	1.83	1.40	11.1	10	12	-2
Mean	0.47	0.93	0.70	6.4	5.6	9	-3

Kelif	ΔTx (°C)	ΔTn (°C)	ΔTmn (°C)	ΔP (%)	ΔQ_T (%)	ΔQ_C (%)	ΔQ_H (%)
1950s	-0.10	0.14	0.02	11.9		8	
1960s	0.20	0.42	0.31	8.5		8	
1970s	0.11	0.47	0.29	2.2		2	
1980s	0.56	0.95	0.75	8.3	-8	6	-15
1990s	0.57	1.00	0.78	13.1	2	15	-13
2000s	1.23	1.78	1.51	14.1	-10	14	-24
2010s	1.04	1.84	1.44	12.8	-32	13	-45
Mean	0.51	0.94	0.73	10.1	-6	10	-16

Doab	ΔTx (°C)	ΔTn (°C)	ΔTmn (°C)	ΔP (%)	ΔQ_T (%)	ΔQ_C (%)	ΔQ_H (%)
1950s	-0.21	0.12	-0.05	15.6		48	
1960s	0.23	0.52	0.37	10.9	58	43	15
1970s	0.33	0.98	0.65	2.8	30	37	-7
1980s	0.51	0.99	0.75	12.1	65	17	48
1990s	0.46	1.00	0.73	15.8	94	23	71
2000s	1.11	2.10	1.61	21.6	122	42	80
2010s	0.97	1.99	1.48	14.1	153	29	124
Mean	0.48	1.10	0.79	13.3	88	34	54

Pull-i-khomri	ΔTx (°C)	ΔTn (°C)	ΔTmn (°C)	ΔP (%)	ΔQ_T (%)	ΔQ_C (%)	ΔQ_H (%)
1950s	-0.15	0.13	-0.01	13.4	23	13	9
1960s	0.28	0.51	0.39	10.4	10	12	-1
1970s	0.27	0.70	0.48	3.7	20	19	1
1980s	0.63	0.96	0.79	11.0	21	24	-3
1990s	0.66	1.05	0.85	13.4	22	24	-2
2000s	1.29	1.98	1.64	20.1	24	40	-15
2010s	1.14	1.93	1.53	14.6	26	29	-4
Mean	0.59	1.04	0.81	12.4	21	23	-2

Kulukh-Tepa	ΔTx (°C)	ΔTn (°C)	ΔTmn (°C)	ΔP (%)	ΔQ_T (%)	ΔQ_C (%)	ΔQ_H (%)
1950s	-0.12	0.12	0.00	12.5	-13	10	-23
1960s	0.26	0.47	0.36	9.1	-16	8	-24
1970s	0.18	0.52	0.35	6.6	-34	14	-48
1980s	0.62	0.95	0.78	9.9	-31	14	-45
1990s	0.68	1.06	0.87	11.7	-34	15	-50
2000s	1.32	1.87	1.60	18.8	-37	25	-63
2010s	1.17	1.91	1.54	14.8	-44	25	-69
Mean	0.59	0.99	0.79	11.9	-30	16	-46

Khorog	ΔTx (°C)	ΔTn (°C)	ΔTmn (°C)	ΔP (%)	ΔQ_T (%)	ΔQ_C (%)	ΔQ_H (%)
1950s	-0.09	0.17	0.04	8.9	-6.0	9	-15
1960s	0.20	0.48	0.34	6.1	-17	8	-25
1970s	0.07	0.49	0.28	-1.4	-7	-2	-5
1980s	0.51	1.04	0.77	-0.2	-11	-1	-10
1990s	0.54	1.11	0.82	12.0		14	
2000s	1.24	1.86	1.55	9.5		9	
2010s	1.01	1.95	1.48	9.6		10	
Mean	0.50	1.01	0.76	6.4	-10	7	-17

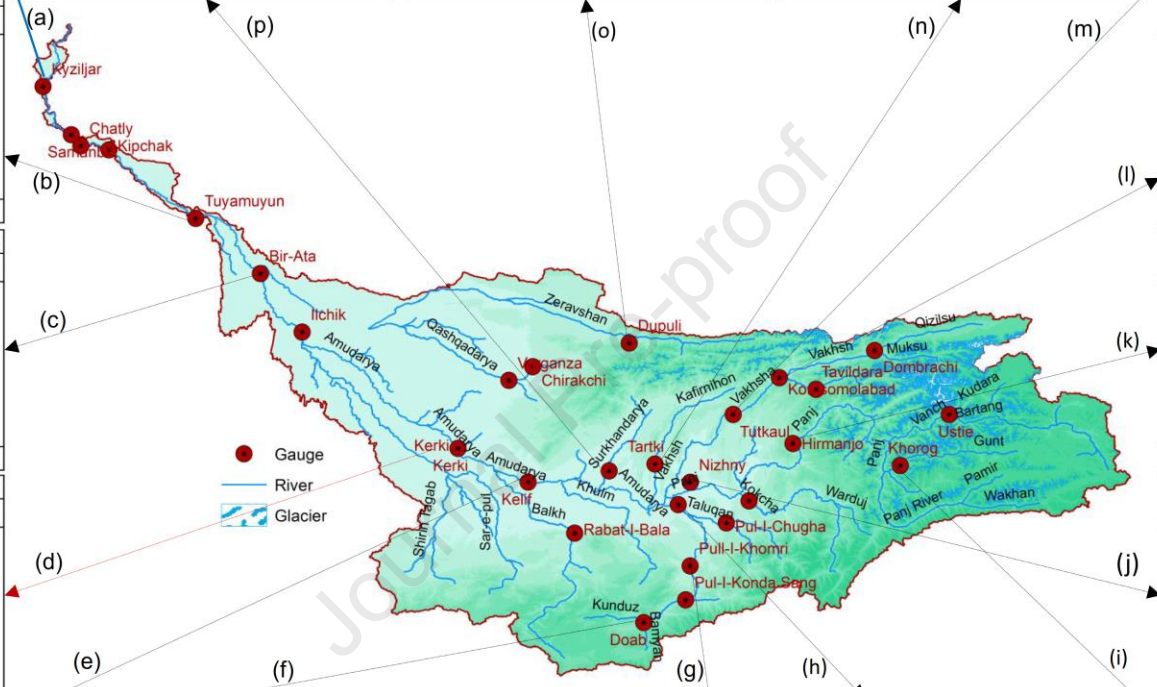

Figure 4. Climatic changes and the impacts of climate change (ΔQ_C), human activities (ΔQ_H), and both (ΔQ_T) on the streamflow of all tributaries in the Amudarya River basin for the impacted period (1951–2020) relative to the baseline period (1931–1950).

4.4 Climate elasticity of streamflow

The Hydrological Modelling Approach (HMA) was used to explore the elasticity of streamflow with respect to precipitation, actual AET, and temperature (E_P, E_{AET}, and E_T, respectively), as shown in Figure 5 (b–d). The statistical indicators (Sankarasubramanian et al. (2001) (S-indicator) and Zheng et al. (2009) (Z-indicator) were used to determine streamflow elasticity to precipitation (E_P) and PET (E_{PET}), as shown in Figure 6 (a–d), at 34 locations (Figure 5a) on the main tributaries in the ADRB.

According to the HMA, E_P, E_{AET}, and E_T ranged from 0.04–3.60, -1.15– -0.03, and -0.02–1.53, with average values of 1.25, -0.17, and 0.31, respectively. This means that, on average, a 10% increase in precipitation and temperature can increase streamflow by 12.5% and 3.1% in the basin. However, a 10% increase in AET can decrease streamflow by 1.7%, indicating that the basin's streamflow is more sensitive to precipitation changes than the other two climate variables. Figure 5b shows that the Kunduz basin (with E_P of 1.57–3.6), Surkhandarya (2.83), Qashqadarya (1.94), and Zeravshan (1.86) are the most sensitive basins to precipitation in the ADRB, which can produce 2 times the streamflow by a unit increase in precipitation. However, the Vakhsh and Kofirnihon River basins were the least sensitive to precipitation. Figure 5c shows a similar distribution for E_{AET}, but in reverse order (decreasing streamflow). For example, the Kunduz basin was most sensitive to precipitation and AET. However, precipitation had a much greater effect on streamflow than AET for the same unit change. In the case of temperature (Figure 5d), it was observed that tributaries such as the Vakhsh, Kokchah, and Panj, which have dominant glacier contributions, were more sensitive to temperature than others. This means these basins can produce more streamflow by increasing temperature, but the glaciers' size will be reduced in the future.

According to the S-indicator, E_P and E_{PET} ranged from 0.49–1.57 and -6.0–-0.62, with mean values of 0.92 and -2.19, respectively. The Z-indicator obtained similar values for E_P and E_{PET}, ranging from 0.48–1.44 and -4.53–-1.22, with mean values of 0.86 and -2.19, respectively. Both indicators showed spatial distributions similar to each other and to the HMA, but with lower $_{EP}$ magnitudes and much higher E_{PET} magnitudes than the modelling approach.

The higher precipitation elasticity estimated using the HMA, compared to the statistical indicator, reflects the model's ability to explicitly represent nonlinear hydrological processes and climate–runoff interactions, particularly those related to snowmelt, evapotranspiration, and basin storage. In contrast, the statistical indicator is based on historical variability and assumes a stationary precipitation–streamflow relationship, which may reduce sensitivity estimates in complex, cryosphere-influenced basins. On the other hand, the much stronger evapotranspiration elasticity estimated using the statistical indicators compared to the HMA mainly reflects

methodological differences, particularly the use of actual evapotranspiration in the model, which is constrained by soil moisture, versus potential evapotranspiration in the statistical indicators, which represents atmospheric demand. Additionally, the model smooths evapotranspiration impacts through basin storage, while statistical indicators directly link evapotranspiration variability to streamflow, potentially overstating its influence in dry basins. In two previous studies, Hu et al. (2021) and Hou et al. (2023) explored E_P and E_{PET} using the Budyko method and the Z-indicator for the periods 1960–2017 and 1974–2015, respectively, at Kerki and Kyzyl-jar. Hu et al. (2021) explored E_P of 1.6 and 2.69 and E_{PET} of -0.62 and -1.66 at Kerki and Kyzyl-jar, and Hou et al. (2023) disclosed E_P of 0.71 and 0.94 and E_{PET} of -0.07 and -0.04 at Kerki and Kyzyl-jar. Our results have a little difference in the case of E_P (e.g., at Kerki /Kyzyl-jar, 0.91/1.06 from the HMA and 0.77/84 from the Z-indicator) but a big difference in the case of E_{PET} (e.g., at Kerki, -0.04/-0.05 from the HMA and -2.25/-2.79 from the Z-indicator). The two possible reasons are the time period of estimation and the streamflow data used for the calculation. For example, we used a longer period (1931–2020) than both studies (i.e., 1960–2017 and 1974–2015). We also utilized simulated naturalized streamflow, as done by Lv et al. (2018), in the lower reaches of the Yellow River instead of observed streamflow. In the basin, streamflow has mainly decreased due to human extraction for irrigation in the lower and middle reaches during 1960–1990 (UNEP, 2011). So, using observed streamflow for climate elasticity analysis can cause misleading results. The E_P results of Hu et al. (2021) using the Budyko water-balance framework are approximately twice those obtained in this study using the HMA. This might be the assumption underlying the elasticity method, which treats changes in water storage as negligible. In addition, the higher E_P reported by Hu et al. (2021) may also reflect the simplified structure of the Budyko framework, which does not explicitly account for snow and glacier melt, groundwater storage, or routing processes. The higher precipitation elasticity reported by Hu et al. (2021) may also be due to their use of observed streamflow rather than naturalized streamflow, as observed discharge reflects not only precipitation variability but also the influence of human activities such as irrigation withdrawals. In contrast, the hydrological modelling approach represents these buffering mechanisms explicitly, leading to more moderated streamflow responses to precipitation variability. Hu et al. (2021) and Hou et al. (2023) only used statistical methods; however, the modelling approach is considered a robust method to explore the climate elasticity of streamflow, though it requires more information (Yang and Yang, 2011). The naturalized streamflow is more suitable for identifying the climate change effects on streamflow (Lv et al., 2018). The HMA can provide realistic estimates of the climate elasticity of streamflow because all other hydrological processes, such as evapotranspiration, snow and glacier melt, canopy storage, suface storage, soil storage, and infiltration, occur simultaneously in a basin.

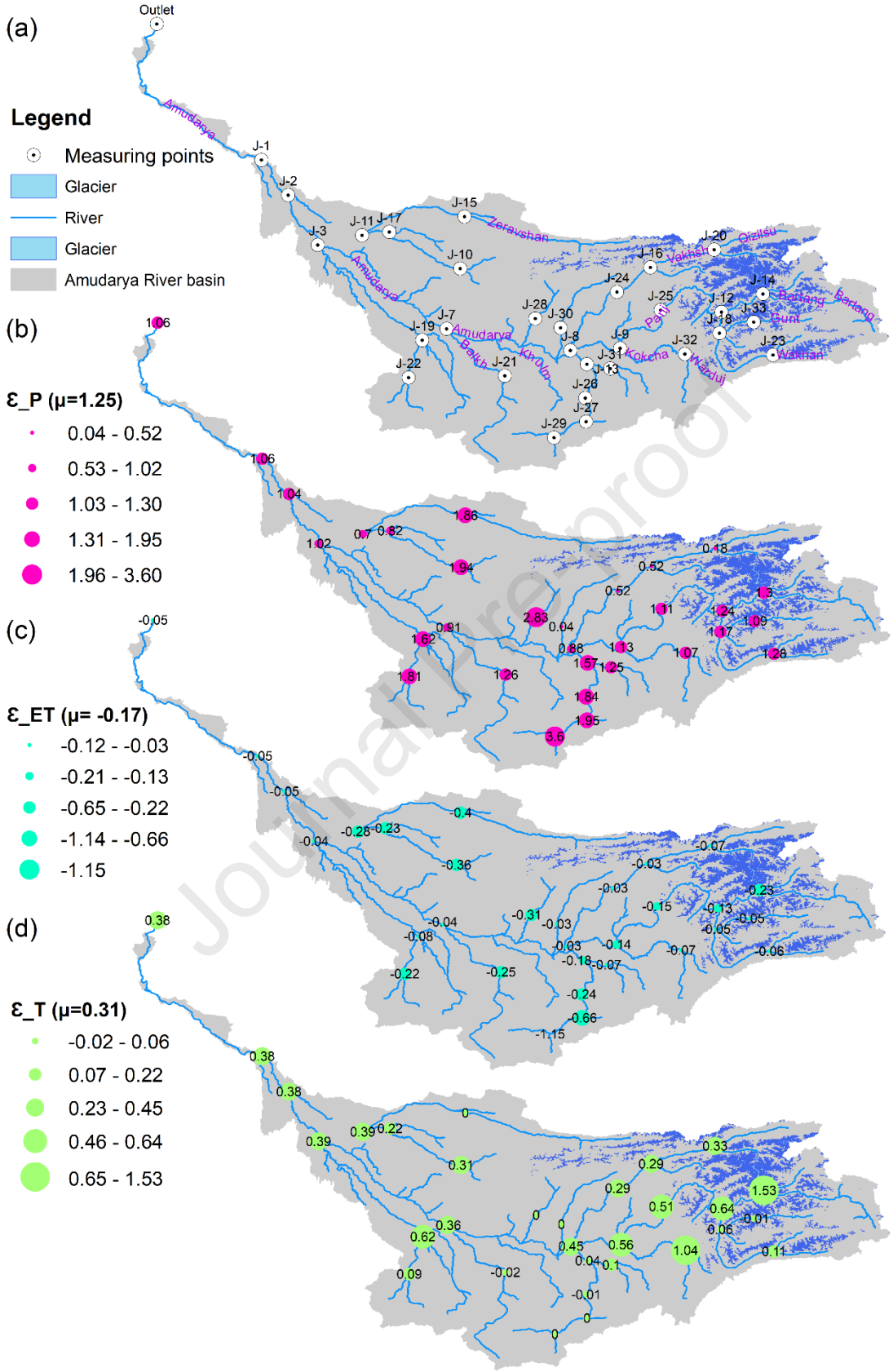

574

575 Figure 5. Climate elasticity of streamflow, a) analysis locations, b) precipitation, c) actual evapotranspiration, and

576 d) mean temperature for all tributaries of the Amudarya river, using the hydrological modelling approach.

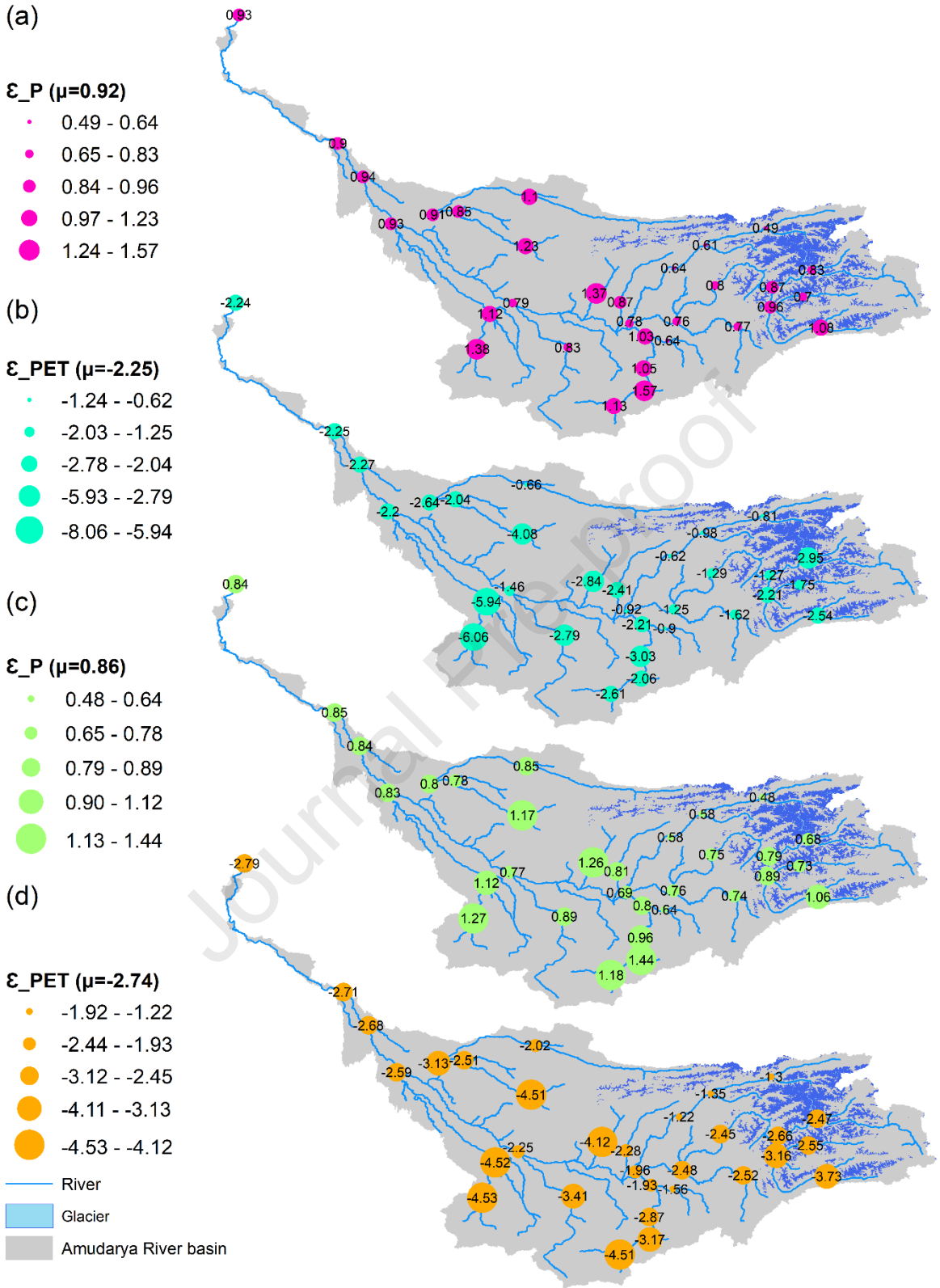

577

578 Figure 6. Precipitation (ε_P) and potential evapotranspiration (ε_PET) elasticity of streamflow for all tributaries

579 of the Amudarya River, using the Sankarasubramanian-indicator (a and b) Zheng-indicator (c and d).

5 Discussion

5.1 Impacts of climate variability on streamflow

This study's results showed that a decrease in basin streamflow is mainly due to HA, not CC, because increased precipitation directly increases streamflow, whereas increased temperature indirectly increases streamflow by melting more glaciers. According to Hou et al. (2023), streamflow in the basin is mainly generated by snow (43%) and glacier melting (39%) in the headwaters of the ADRB. This means CC, especially an increase in temperature, is a big challenge in the basin, which will cause more streamflow by melting, but for a shorter period. Glaciers are projected to decrease by about 50% by 2050 relative to 2010, resulting in reduced streamflow thereafter (Immerzeel et al., 2012). According to Hagg et al. (2013), by 2050, under temperature increases of 2.2°C and 3.1°C, glacier extents in the Rukhk river (a small tributary of Amudarya) are projected to decrease by 36% and 45%, respectively. This reduction is significant, especially in lower elevation zones where glaciers may disappear almost entirely. These alterations in upstream glaciers will impact hydrological processes in the ADRB, including shifts in seasonal runoff, changes in peak runoff timing, and a long-term decline in water availability. Glacier alterations will not only influence the quantity of water but also critically affect its seasonal distribution, posing challenges for water resource management and agricultural planning in the Amu Darya Basin (Chen et al., 2017; Hagg et al., 2013).

However, in the lowland areas of the basin, which already have low annual rainfall (100–200 mm)(Salehie et al., 2021), the increased temperature will trigger evapotranspiration, reducing the amount of water reaching the main river streams. Although CC had no impact on streamflow reduction, as shown in Figure 7 (discussed below), it will alter the basin's hydrologic regime and reduce streamflow when there is no glacier due to increasing global warming.

5.2 Impacts of human activities on streamflow

Generally, watersheds are more sensitive to external stressors, and their impacts are more damaging in arid and semi-arid regions (Huang et al., 2021), as observed in this study, where human activities caused a profound decrease in streamflow across most tributaries. The main reasons for this are the increasing population, water withdrawal for agriculture, industrial, and domestic purposes, and the construction of dams, headworks, and barrages in the basin. According to UNEP (2011), from 1950 to 1990, the Soviet Union invested substantially in establishing an extensive network of irrigation canals, dams, and pumping stations across Central Asia. Most rivers, such as the Amudarya and Syrdarya, were diverted for irrigated agriculture to produce cotton, wheat, rice, etc., in the arid plains and even desert areas, without regard for ecological requirements. During this era, irrigated

land expanded by about 150% and 130% in the ADRB and Syrdarya basin, respectively (World-Bank, 2004). It is also reported that the network of irrigation canals extended into the deep deserts and covered about 7.6 million hectares of land in the middle and lower reaches located in Turkmenistan and Uzbekistan (UNEP, 2011). The largest irrigation canal, the Karakum (or Garagum) canal, is also constructed on the Amudarya near Kerki, diverting about 15% of the river's flow (Brite, 2018). According to Schlüter et al. (2013), irrigated agriculture consumes about 92% of the Amudarya's streamflow. According to FAO (2021), 30 reservoirs have been constructed in the ADRB, of which 26 were built only between 1950 and 1990 (Table S-1, Supplementary). These reservoirs are mainly used for irrigation, followed by power generation. Thus, the water withdrawal for agriculture is the major factor reducing the streamflow, especially in the middle and lower reaches of the ADR. Hou et al. (2023) and Hu et al. (2021) also concluded that the decrease in streamflow in the basin was mainly due to HA. Hu et al. (2021) reported that HA and CC contributed about 112% and -14% at Kerki and 103% and -4% at Kyzyl-jar, respectively, for 1975–2017 relative to 1960–1974, and Hou et al. (2023) showed contributions of HA and CC of 122% and -22% at Kerki and 107% and -7% at Kyzyl-jar, respectively, for 1974–2015 relative to 1956–1973, which are very similar to our results at these two sites but lower in magnitude. For example, at Kyzyl-jar (Kerki), HA and CC contributed about 114% (144%) and -14% (-44%) in this study. This can be mainly because different climatic datasets, methods, and data periods are used. For example, they used 1960–1974 and 1956–1974 as the BLP, but we used 1931–1950. In this case, our results can be more robust because human activities are not ignorable during their BLPs in these studies, especially in the lower reaches. For example, Figure 4a shows that streamflow decreased by 27% and 57% in the 1950s (1951–1960) and 1960s (1961–1970), respectively, due to the combined effect of CC and HA, at Kyzyl-jar, and Figure 4d shows 9% and 26% decreases in streamflow at Kerki in the 1960s and 1970s, respectively. Therefore, these periods cannot be used as baseline periods. Nonetheless, these periods can be used as BLPs for gauges in the headwaters, such as Doab, Ustie, Khorog, and Khojagar. To understand the impacts of HA and CC on the streamflow in more detail, we calculated annual changes in streamflow due to HA, CC, and both (HA and CC) along with changes in precipitation for the period of 1951–2020 relative to the 1931–1950 at Kyzyl-jar and Kerki, as show in Figure 7. This shows that CC caused an increase in streamflow, with slight upward trend while HA resulted in a decrease in streamflow, with sharp downward trend. It can be seen that decrease in streamflow due both factors is less than the decrease due to HA because of increase in streamflow due to CC. Figure 7 also shows that at lower and middle reaches (below Kerki) the extraction of water is much higher than in the headwater regions. Furthermore, Figure 7, shows clear alterations in streamflow regimes due to HA, which requires to consider proper water resources planning and

management to create a balance between the environment and human needs. Central Asian countries have already endeavoured to deal with water related issue by developing different institutions and organizations such as the International Fund for Saving the Aral Sea, Interstate Commission for Water Coordination of Central Asia, Water Users Association, and the informal Water Users Groups. However, minor effects have been observed on the ground due to various limitations, including a lack of funds and technical support (Abdullaev et al., 2010).

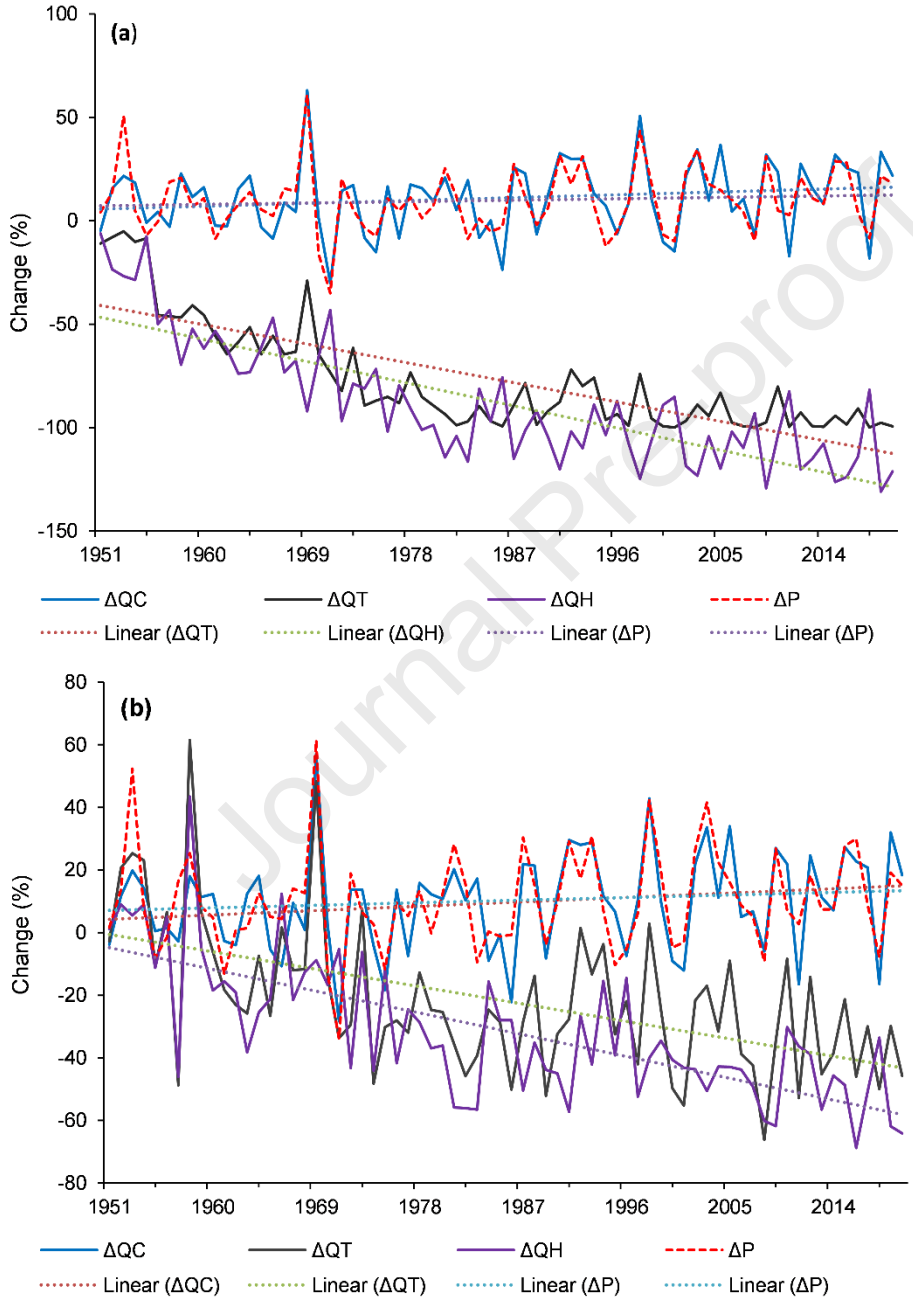

Figure 7. Change in streamflow due to climate change (ΔQC), human activities (ΔQH), and both (ΔQT), as well as change in precipitation (ΔP) at (a) Kyzyl-jar and (b) Kerki for the impacted period (1951–2020) relative to the baseline period (1931–1950).

5.3 Uncertainties, limitations, and suggestions

In impact assessment studies, uncertainties arise from various factors, including data quality, methodology, model structure, and parameter values (Bosshard et al., 2013). According to Chen et al. (2017), the main sources of uncertainty in assessing the regional hydrological impacts of climate change can be unreliable and incomplete datasets. Due to insufficient observed gauged data, CRU-JRA climatic data was used in most analyses across the basin. This represents the first major source of uncertainty in the study. The second source of uncertainty arises from selecting the BLP, which is intended to represent conditions with minimal human interference.

Although we selected 1931–1950 as a BLP, considering all possible factors, there remain sources of uncertainty. A third source of uncertainty stems from the simplified representation of hydrological processes in the hydrological model. For example, due to a lack of climate and snow/ice data, the Temperature Index method was used to account for melting water rather than the Energy Balance Method. HEC-HMS does not explicitly quantify the separate contributions of snow and glacier melt to streamflow; instead, it represents snow and ice melt indirectly, which limits the ability to analyze meltwater contributions independently. The uncertainties associated with hydrological models also influence climate impact studies (Faiz et al., 2018). Generally, uncertainties in hydrological modelling are associated with input data, output data, model structure, and estimated parameters (Renard et al., 2010).

The present study provides the latest and most comprehensive novel results, both temporally and spatially, across the basin for almost all tributaries, which can be used to understand hydrological responses to changing climate and human activities and to manage water resources in the ADRB. It is recommended that more efficient technologies be adopted to mitigate human impacts on regional water resources, while strengthening alignment with the United Nations Sustainable Development Goals related to climate action (SDG 13) and clean water and sanitation (SDG 6).

6 Conclusions

The Amudarya River, the largest river basin in Central Asia, has been severely altered by human activities (e.g., the construction of irrigation canals, dams, and headworks) to meet human needs, resulting in almost no water for the Aral Sea, which was the 4th-largest lake in the world in the 1960s. Climate change and global warming pose significant threats to water resources and their availability in the basin, as the river is primarily fed by snowfall and glaciers. The present study used the hydrological modelling approach to separate and quantify the impacts of climate change and human activities on streamflow, along with climate elasticity. The elasticity was also determined using statistical indicators (S- and Z-Indicators). The analyses were performed for the period 1931–

2020 at 25–34 points, with 1931–1950 serving as the BLP and 1951–2020 as the IPP. The main challenge in this study was to calibrate HEC-HMS between 1931 and 1950 due to the scarcity and low quality of hydroclimatic data, which were obtained from various institutions, including the Climate Research Unit, Global Runoff Data Centre, and Scientific Information Centre.

The results indicate pronounced climatic changes in the region during the impacted period (IPP) relative to the baseline period (BLP). Over this period, Tmax, Tmin, and Tmean increased by 0.45 °C, 0.88 °C, and 0.67 °C, respectively, while precipitation increased by 9.8%. Both climate change and human activities substantially altered streamflow dynamics. Overall, streamflow in the basin (at the outlet) declined by 77%, with human activities accounting for a −114% contribution to the decline, offsetting the positive contribution from climate change (14%). In the headwater regions, streamflow decreased by 22%, with human activities contributing −145% of the decrease, offsetting the positive effects (45%) of climate change. The main tributaries, including the Panj and Vakhsh rivers, experienced streamflow reductions ranging from 0.4% to 34%, primarily attributed to human activities. In contrast, the headwaters of the Panj (e.g., Nizhny), Kunduz (e.g., Doab and Pull-I-Khomri), and Vakhsh (e.g., Komsomolabad and Garam) showed increases in streamflow, mainly due to climate change (increased precipitation and temperature). Overall, human activities were the dominant factor driving reductions in streamflow across all major tributaries, ultimately leading to decreased water inflow to the delta and the Aral Sea. Climate elasticity analysis indicated that precipitation had the strongest control on streamflow variability among all climatic variables.

This study shows that human activities contributed overwhelmingly to reductions in streamflow across the basin, underscoring the urgent need to modernize irrigation systems, reduce conveyance losses, and support efficient water-use technologies. Strengthening transboundary water governance through enhanced collaboration, data sharing, and institutional support is essential, alongside aligning basin-wide strategies with the Sustainable Development Goals. Improved hydroclimatic monitoring—including expanded gauging networks, glacier and snow-cover observations, and remote sensing capabilities—will support more reliable future assessments. Long-term water planning must also integrate climate change impacts, encourage adaptive reservoir operations, promote water-efficient cropping patterns, and safeguard environmental flows to restore the degraded Amudary delta and the Aral Sea ecosystems.

Acknowledgements:

We sincerely thank the Alliance of International Science Organisations (ANSO) Collaborative Research Project Fund (ANSO-CR-PP-2022-06) for their financial support. We are also grateful to the Chinese Academy of

Sciences (E44S0200) and the Institute of Geographic Sciences and Natural Resources Research, Chinese Academy of Sciences (E3V30030). Additionally, we extend our appreciation to the Princeton Meteorological Dataset and the Global Historical Climatology Network for providing open-access meteorological data and to the Global Runoff Data Centre (GRDC) for streamflow observations.

Conflict of interest: The authors declare that they have no conflicts of interest.

Data availability statement: The monthly hydrological data applied in this study are available at the Central Asia Water Portal (http://www.cawater-info.net/). In contrast, daily streamflow data is placed at the Global Runoff Data Center (www.bafg.de/GRDC/). Climatic data can be obtained freely from the Climate Research Unit (Harris and UEA-CRU, 2023) at https://catalogue.ceda.ac.uk/uuid/43ce517d74624a5ebf6eec5330cd18d5.

Other open-source data, such as elevation, land cover, and soil datasets, are available at NASA (http://srtm.csi.cgiar.org), the Climate Change Initiative Land Cover (CCI-LC) product produced by the European Space Agency (https://www.esa-landcover-cci.org/), and the Harmonised World Soil Database (Fischer et al., 2008), respectively. The initial glacier distribution dataset can be obtained from the Randolph Glacier Inventory (RGI) 4.0 (RGI-Consortium, 2017).

References

Abdullaev, I., Kazbekov, J., Manthritilake, H., Jumaboev, K., 2010. Water User Groups in Central Asia: Emerging form of collective action in irrigation water management. Water Resources Management, 24(5): 1029-1043. https://doi.org/10.1007/s11269-009-9484-4.

Ahbari, A., Stour, L., Agoumi, A., Serhir, N., 2018. Estimation of initial values of the HMS model parameters: Application to the basin of Bin El Ouidane (Azilal, Morocco). Journal of Materials and Environmental Science, 9(1): 305-317. https://doi.org/10.26872/jmes.2018.9.1.34.

Akhundzadah, N.A., Soltani, S., Aich, V., 2020. Impacts of climate change on the water resources of the Kunduz River basin, Afghanistan, Climate. https://doi.org/10.3390/cli8100102.

Anderson, B.J., Brunner, M.I., Slater, L.J., Dadson, S.J., 2024. Elasticity curves describe streamflow sensitivity to precipitation across the entire flow distribution. Hydrol. Earth Syst. Sci., 28(7): 1567-1583. 10.5194/hess-28-1567-2024.

Araghi, A., Martinez, C.J., 2024. Evaluation of CRU-JRA gridded meteorological dataset for modeling of wheat production systems in Iran. International Journal of Biometeorology, 68(6): 1201-1211. 10.1007/s00484-024-02659-9.

Armstrong, R.L. et al., 2019. Runoff from glacier ice and seasonal snow in High Asia: Separating melt water sources in river flow. Regional Environmental Change, 19(5): 1249-1261. https://doi.org/10.1007/s10113-018-1429-0.

Bosshard, T. et al., 2013. Quantifying uncertainty sources in an ensemble of hydrological climate-impact projections. Water Resources Research, 49(3): 1523-1536. https://doi.org/10.1029/2011WR011533.

Brite, E.B., 2018. The hydrosocial empire: The Karakum River and the Soviet conquest of Central Asia in the 20th century. Journal of Anthropological Archaeology, 52: 123-136. https://doi.org/10.1016/j.jaa.2018.08.003.

Chen, Y., Li, W., Fang, G., Li, Z., 2017. Review article: Hydrological modeling in glacierized catchments of central Asia – status and challenges. Hydrol. Earth Syst. Sci., 21(2): 669-684. http://dx.doi.org/10.5194/hess-21-669-2017.

Chiew, F.H., Peel, M.C., McMahon, T.A., Siriwardena, L.W., 2006. Precipitation elasticity of streamflow in catchments across the world. In: Demuth, S., Gustard, A., Planos, E., Scatena, F., Servat, E. (Eds.),

CLIMATE VARIABILITY AND CHANGE - HYDROLOGICAL IMPACTS. International Association of Hydrological Sciences (IAHS), Havana, Cuba, pp. 308.

Coe, M.T., Latrubesse, E.M., Ferreira, M.E., Amsler, M.L., 2011. The effects of deforestation and climate variability on the streamflow of the Araguaia River, Brazil. Biogeochemistry, 105(1): 119-131. http://dx.doi.org/10.1007/s10533-011-9582-2.

Dariane, A.B., Javadianzadeh, M.M., James, L.D., 2016. Developing an Efficient Auto-Calibration Algorithm for HEC-HMS Program. Water Resources Management, 30(6): 1923-1937. 10.1007/s11269-016-1260-7.

Dey, P., Mishra, A., 2017. Separating the impacts of climate change and human activities on streamflow: A review of methodologies and critical assumptions. Journal of Hydrology, 548: 278-290. https://doi.org/10.1016/j.jhydrol.2017.03.014.

Di Baldassarre, G., Montanari, A., 2009. Uncertainty in river discharge observations: A quantitative analysis. Hydrology and Earth System Sciences, 13(6): 913-921. http://dx.doi.org/10.5194/hess-13-913-2009.

Faiz, M.A. et al., 2018. Performance evaluation of hydrological models using ensemble of General Circulation Models in the northeastern China. Journal of Hydrology, 565: 599-613. https://doi.org/10.1016/j.jhydrol.2018.08.057.

FAO, 2021. Geo-referenced point database on dams in Central Asia. In: (FAO), A. (Ed.). Food and Agriculture Organization of the United Nations.

Finger, D., Pellicciotti, F., Konz, M., Rimkus, S., Burlando, P., 2011. The value of glacier mass balance, satellite snow cover images, and hourly discharge for improving the performance of a physically based distributed hydrological model. Water Resources Research, 47(7). https://doi.org/10.1029/2010WR009824.

Fischer, G. et al., 2008. Global Agro-ecological Zones Assessment for Agriculture (GAEZ 2008). In: IIASA, L., Austria and FAO, Rome, Italy. (Ed.). FAO.

Garna, R.K., Fuka, D.R., Faulkner, J.W., Collick, A.S., Easton, Z.M., 2023. Watershed model parameter estimation in low data environments. Journal of Hydrology: Regional Studies, 45: 101306. https://doi.org/10.1016/j.ejrh.2022.101306.

Gilbert, N., 2012. Water under pressure. Nature, 483(7389): 256-257. https://doi.org/10.1038/483256a.

Hagg, W., Hoelzle, M., Wagner, S., Mayr, E., Klose, Z., 2013. Glacier and runoff changes in the Rukhk catchment, upper Amu-Darya basin until 2050. Global and Planetary Change, 110: 62-73. https://doi.org/10.1016/j.gloplacha.2013.05.005.

Harris, I., Osborn, T.J., Jones, P., Lister, D., 2020. Version 4 of the CRU TS monthly high-resolution gridded multivariate climate dataset. Scientific Data, 7(1): 109. https://doi.org/10.1038/s41597-020-0453-3.

Harris, I.C., UEA-CRU, 2023. CRU JRA v2.5: A forcings dataset of gridded land surface blend of Climatic Research Unit (CRU) and Japanese reanalysis (JRA) data; Jan. 1901 – Dec. 2023. In: (CEDA), N.E.C.f.E.D.A. (Ed.). University of East Anglia Climatic Research Unit.

He, H. et al., 2022. Numerical study on the climatic effect of the Aral Sea. Atmospheric Research, 268: 105977. https://doi.org/10.1016/j.atmosres.2021.105977.

Hou, M. et al., 2023. Streamflow composition and the contradicting impacts of anthropogenic activities and climatic change on streamflow in the Amu Darya Basin, Central Asia. Journal of Hydrometeorology, 24(2): 185-201. https://doi.org/10.1175/JHM-D-22-0040.1.

Hu, Y. et al., 2021. An integrated assessment of runoff dynamics in the Amu Darya River basin: Confronting climate change and multiple human activities, 1960–2017. Journal of Hydrology, 603: 126905. https://doi.org/10.1016/j.jhydrol.2021.126905.

Hu, Z., Wang, L., Wang, Z., Hong, Y., Zheng, H., 2015. Quantitative assessment of climate and human impacts on surface water resources in a typical semi-arid watershed in the middle reaches of the Yellow River from 1985 to 2006. Int. J. Climatol., 35(1): 97-113. https://doi.org/10.1002/joc.3965.

Huang, W., Duan, W., Chen, Y., 2021. Rapidly declining surface and terrestrial water resources in Central Asia driven by socio-economic and climatic changes. Science of The Total Environment, 784: 147193. https://doi.org/10.1016/j.scitotenv.2021.147193.

Immerzeel, W.W., Lutz, A., Droogers, P., 2012. Climate Change Impacts on the upstream water resources of the Amu and Syr Darya River basins. Report Future Water: 107, Future Water, Wageningen, The Netherlands.

IPCC, 2022. Climate Change 2021: Summary for All. WORKING GROUP I TECHNICAL SUPPORT UNIT, WMO, UNEP, and IPCC.

Kan, G. et al., 2019. Computer aided numerical methods for hydrological model calibration: an overview and cecent development. Archives of Computational Methods in Engineering, 26(1): 35-59. https://doi.org/10.1007/s11831-017-9224-5.

Keller, A.A., Garner, K., Rao, N., Knipping, E., Thomas, J., 2023. Hydrological models for climate-based assessments at the watershed scale: A critical review of existing hydrologic and water quality models. Science of The Total Environment, 867: 161209. https://doi.org/10.1016/j.scitotenv.2022.161209.

Kobayashi, S. et al., 2015. The JRA-55 Reanalysis: General Specifications and Basic Characteristics. Journal of the Meteorological Society of Japan. Ser. II, 93(1): 5-48. 10.2151/jmsj.2015-001.

Kure, S., Jang, S., Ohara, N., Kavvas, M.L., Chen, Z.Q., 2013. Hydrologic impact of regional climate change for the snowfed and glacierfed river basins in the Republic of Tajikistan: hydrological response of flow to climate change. Hydrological Processes, 27(26): 4057-4070. https://doi.org/10.1002/hyp.9535.

Levy, M., Lopes, A., Cohn, A., Larsen, L., Thompson, S., 2018. Land use change increases streamflow across the arc of deforestation in Brazil. Geophysical Research Letters, 45. https://doi.org/10.1002/2017GL076526.

Li, Z., Li, Q., Wang, J., Feng, Y., Shao, Q., 2020. Impacts of projected climate change on runoff in upper reach of Heihe River basin using climate elasticity method and GCMs. Science of The Total Environment, 716: 137072. https://doi.org/10.1016/j.scitotenv.2020.137072.

Lioubimtseva, E., 2014. Impact of climate change on the Aral Sea and its basin. In: Micklin, P., Aladin, N.V., Plotnikov, I. (Eds.), The Aral Sea: The Devastation and Partial Rehabilitation of a Great Lake. Springer Berlin Heidelberg, Berlin, Heidelberg, pp. 405-427. https://doi.org/10.1007/978-3-642-02356-9_17.

Lv, M., Ma, Z., Lv, M., 2018. Effects of climate/land surface changes on streamflow with consideration of precipitation intensity and catchment characteristics in the Yellow River Basin. Journal of Geophysical Research: Atmospheres, 123(4): 1942-1958. https://doi.org/10.1002/2017JD027625.

Mahmood, R., Jia, S., 2019. Assessment of hydro-climatic trends and causes of dramatically declining stream flow to Lake Chad, Africa, using a hydrological approach. Science of The Total Environment. https://doi.org/10.1016/j.scitotenv.2019.04.219.

Mahmood, R., Jia, S., 2022. A Comprehensive Approach to Develop a Hydrological Model for the Simulation of All the Important Hydrological Components: The case of the Three-River Headwater Region, China, Water. https://doi.org/10.3390/w14182778.

Mahmood, R. et al., 2025. Developing a Multimodel Ensemble Framework for Improved Streamflow Simulation in the Amudarya River Basin. Journal of Hydrometeorology, 26(11): 1693-1716. https://doi.org/10.1175/JHM-D-25-0055.1.

Mahmood, R., Jia, S., Lv, A., Naeem, S., 2024. Environmental flow assessment, evaluation, and suggestions for dying riverine ecosystem of the transboundary Amudarya River, Central Asia. Ecological Indicators, 158: 111419. https://doi.org/10.1016/j.ecolind.2023.111419.

Mahmood, R., Jia, S., Lv, A., Zhu, W., 2020. A preliminary assessment of environmental flow in the three rivers' source region, Qinghai Tibetan Plateau, China and suggestions. Ecological Engineering, 144: 105709. https://doi.org/10.1016/j.ecoleng.2019.105709.

Mahmood, R., Jia, S., Zhu, W., 2019. Analysis of climate variability, trends, and prediction in the most active parts of the Lake Chad basin, Africa. Scientific Reports, 9(1): 6317. https://doi.org/10.1038/s41598-019-42811-9.

Menne, M.J., Durre, I., Vose, R.S., Gleason, B.E., Houston, T.G., 2012. An overview of the Global Historical Climatology Network-daily database. Journal of Atmospheric and Oceanic Technology, 29(7): 897-910. https://doi.org/10.1175/JTECH-D-11-00103.1.

Moriasi, D., Gitau, M., Pai, N., Daggupati, P., 2015. Hydrologic and water quality models: Performance measures and evaluation criteria. Transactions of the ASABE (American Society of Agricultural and Biological Engineers), 58: 1763-1785. https://doi.org/10.13031/trans.58.10715.

Murodov, A. et al., 2023. Extreme hydrometeorological conditions and changes in the Amu Darya River Basin in Central Asia. Journal of Hydrometeorology, 24(2): 315-334. https://doi.org/10.1175/JHM-D-22-0025.1.

Nachtergaele, F.O. et al., 2012. *Harmonized World Soil Database (version 1.2)*. Food and Agriculture Organization of the UN, International Institute for Applied Systems Analysis, ISRIC - World Soil Information, Institute of Soil Science - Chinese Academy of Sciences, Joint Research Centre of the EC, Laxenburg, Austria.

Renard, B., Kavetski, D., Kuczera, G., Thyer, M., Franks, S.W., 2010. Understanding predictive uncertainty in hydrologic modeling: The challenge of identifying input and structural errors. Water Resources Research, 46(5): 1-22. 10.1029/2009WR008328.

RGI-Consortium, 2017. Randolph Glacier Inventory - A dataset of global glacier outlines, version 6. National Snow and Ice Data Center, Boulder, Colorado USA.

Salehie, O. et al., 2021. Ranking of gridded precipitation datasets by merging compromise programming and global performance index: a case study of the Amu Darya basin. Theor Appl Climatol, 144(3): 985-999. https://doi.org/10.1007/s00704-021-03582-4.

Salehie, O. et al., 2022a. Assessment of water resources availability in Amu Darya River Basin using GRACE Data, Water. https://doi.org/10.3390/w14040533.

Salehie, O. et al., 2022b. Selection of the gridded temperature dataset for assessment of thermal bioclimatic environmental changes in Amu Darya River basin. Stochastic Environmental Research and Risk Assessment, 36(9): 2919-2939. https://doi.org/10.1007/s00477-022-02172-8.

Sankarasubramanian, A., Vogel, R.M., Limbrunner, J.F., 2001. Climate elasticity of streamflow in the United States. Water Resources Research, 37(6): 1771-1781. https://doi.org/10.1029/2000WR900330.

Schaefli, B., Huss, M., 2011. Integrating point glacier mass balance observations into hydrologic model identification. Hydrol. Earth Syst. Sci., 15(4): 1227-1241. https://doi.org/10.5194/hess-15-1227-2011.

Schlüter, M. et al., 2013. Enhancing resilience to water flow uncertainty by integrating environmental flows into water management in the Amudarya River, Central Asia. Global and Planetary Change, 110: 114-129. https://doi.org/10.1016/j.gloplacha.2013.05.007.

SIC-ICWC, 2025. Water resources of Amu Darya River basin. Scientific-Information Center of the Interstate Coordination Water Commission (SIC-ICWC).

Singh, S. et al., 2023. Global distribution of pesticides in freshwater resources and their remediation approaches. Environmental Research, 225: 115605. https://doi.org/10.1016/j.envres.2023.115605.

Sterner, R.W. et al., 2020. Ecosystem services of Earth's largest freshwater lakes. Ecosystem Services, 41: 101046. https://doi.org/10.1016/j.ecoser.2019.101046.

Tobias Siegfried, B.M., Adrian Kreiner, and Aidar Zhumabaev, 2024. Climate data in Part II: Data Sources, Retrieval and Preparation, Modeling of Hydrological Systems in Semi-Arid Central Asia. hydrosolutions GmbH, Zenodo. https://doi.org/10.5281/zenodo.6349984.

UNEP, 2003. *Afghanistan: Post-conflict environmental assessment*, 1, Geneva, Switzerland, 180 pp.

UNEP, 2011. Environment and security in the Amu Darya Basin, UNEP, UNDP, UNECE, OSCE, REC, NATO, France.

USACE, 2023. *Hydrologic Modeling System: HEC-HMS User's Manual Version 4.11*. Hydrologic Engineering Center, Davis, California, USA, 843 pp.

Varzi, M., Wegerich, K., 2008. Much ado about nothing – Sub-Basin Working Groups in Kunduz River Basin, pp. 47-61.

Viala, E., 2008. Water for food, water for life a comprehensive assessment of water management in agriculture. Irrigation and Drainage Systems, 22(1): 127-129. https://doi.org/10.1007/s10795-008-9044-8.

Wang, G., Zhang, J., He, R., Jiang, N., Jing, X.a., 2008. Runoff reduction due to environmental changes in the Sanchuanhe river basin. International Journal of Sediment Research, 23(2): 174-180. https://doi.org/10.1016/S1001-6279(08)60017-7.

Wang, L. et al., 2025. Impact of topography and meteorological forcing on snow simulation in the Canadian Land Surface Scheme Including Biogeochemical Cycles (CLASSIC). EGUsphere, 2025: 1-37. 10.5194/egusphere-2025-1264.

Wang, W. et al., 2013. Quantitative assessment of the impact of climate variability and human activities on runoff changes: a case study in four catchments of the Haihe River basin, China. Hydrological Processes, 27(8): 1158-1174. 10.1002/hyp.9299.

Wang, X. et al., 2020. The impact of climate change and human activities on the Aral Sea Basin over the past 50 years. Atmospheric Research, 245: 105125. https://doi.org/10.1016/j.atmosres.2020.105125.

Wang, X. et al., 2016. Attribution of runoff decline in the Amu Darya River in Central Asia during 1951–2007. Journal of Hydrometeorology, 17(5): 1543-1560. https://doi.org/10.1175/JHM-D-15-0114.1.

White, C.J., Tanton, T.W., Rycroft, D.W., 2014. The impact of climate change on the Water Resources of the Amu Darya Basin in Central Asia. Water Resources Management, 28(15): 5267-5281. https://doi.org/10.1007/s11269-014-0716-x.

World-Bank, 2004. Water Energy Nexus in Central Asia: Improving regional cooperation in the Syr Darya Basin., Washington, D.C.

Xu, Z.P., Li, Y.P., Huang, G.H., Wang, S.G., Liu, Y.R., 2021. A multi-scenario ensemble streamflow forecast method for Amu Darya River Basin under considering climate and land-use changes. Journal of Hydrology, 598: 126276. https://doi.org/10.1016/j.jhydrol.2021.126276.

Yang, H., Yang, D., 2011. Derivation of climate elasticity of runoff to assess the effects of climate change on annual runoff. Water Resources Research, 47(7). https://doi.org/10.1029/2010WR009287.

Yin, C. et al., 2025. CETD, a global compound events detection and visualisation toolbox and dataset. Scientific Data, 12(1): 356. 10.1038/s41597-025-04530-x.

Zheng, H. et al., 2009. Responses of streamflow to climate and land surface change in the headwaters of the Yellow River Basin. Water Resources Research, 45(7). https://doi.org/10.1029/2007WR006665.

Declaration of interests

☒ The authors declare that they have no known competing financial interests or personal relationships that could have appeared to influence the work reported in this paper.

☐ The author *Click here to enter your name* is Choose an item for *Click here to enter the journal's name* and was not involved in the editorial review or the decision to publish this article.

☐The authors declare the following financial interests (e.g., any funding for the research project)/personal relationships (e.g., the author is an employee of a profitable company) which may be considered as potential competing interests:

Click here to enter your full declaration